TECHNISCHE
UNIVERSITÄT
WIEN
Vienna University of Technology

D I P L O M A R B E I T

Pharmacological intervention in MYCN amplified human neuroblastoma cell lines

Ausgeführt am Institut für Verfahrenstechnik, Umwelttechnik und Technische

Biowissenschaften der Technischen Universität Chemie

unter der Anleitung von

Ao.Prof. Dr. Martin Hohenegger

durch

Judith Frei
Kalvarienberggasse 70/14

1170 Wien

Wien, März 2015

Danksagung

Bei dem Verfassen einer Diplomarbeit braucht es viel Durchhaltevermögen. Die Unterstützung von Betreuern, Familie und Freunden hat mir die Prozedur um ein Vielfaches erleichtert. Diesen Personen möchte ich hiermit danken!

Ein großer Dank gilt Prof. Dr. Martin Hohenegger, durch den ich einen Einblick in die medizinische Forschung bekommen habe und der die Arbeit immer mit Geduld, Hingabe und fachlicher Kompetenz betreut hat.

Weiteres möchte ich Prof. Dr. Robert Mach vielmals danken, der mir ermöglicht hat, für meine Abschlussarbeit außerhalb der TU zu arbeiten und mich immer in allen organisatorischen Fragen unterstützt hat.

Bei Mag. Christine Wasinger will ich mich bedanken für die Erfahrungen und Tipps, die sie mit mir geteilt hat und mit denen sie mir im Labor zur Seite gestanden hat.

Den größten Dank möchte ich hier aber meinen Eltern aussprechen. Meiner Mutter, die immer zuhört und für mich da ist, die aber in den wesentlichen Augenblicken auch mit ihrer ehrlichen Meinung nicht zurückhält. Und ein großes Dankeschön an meinen Vater, der mir durch seine finanzielle Unterstützung das Studium erst ermöglich hat und mir damit auch immer wieder gezeigt hat, dass er an mich glaubt. I bin froah, dass i enk hon!

1   Content

2 Zusammenfassung

Neuroblastom ist eine unvorhersehbar heterogen verlaufende Tumorerkrankung. MYCN Amplifikation wurde als einer der wenigen konsistenten genetischen Marker beschrieben, welcher mit schlechten Prognosen für den Patienten korreliert. Verschiedene Komponenten werden vermutet beim Prozess der Stabilisierung des Transkriptionsfaktors N-Myc beteiligt zu sein, welcher zu hohen intrazellulären Konzentrationen führt. Das ist der Grund weshalb diese Komponenten als vielversprechende Angriffsziele für eine pharmakologische Intervention gegen die bösartige Krankheit gelten.

Das Hauptziel dieser Studie war es, die Effekte von ausgewählten Substanzen auf die Viabilität und Apoptose in drei primären humanen Neuroblastom Zelllinien zu untersuchen. Die SH-SY5Y Zelllinie ist nicht MYCN amplifiziert und wurde als Kontrolle mit den amplifizierten Kelly und IMR-32 Zelllinien verglichen. Außerdem wurden die Substanzen auch in zweifachen Kombinationen miteinander eingesetzt, um mögliche additive oder synergistische Effekte zu identifizieren. Der HMG-CoA Reduktase Inhibitor Simvastatin, der Aurorakinase A Inhibitor VX680, der Anaplastische Lymphomkinase (ALK) Inhibitor TAE684 und der Histondeacetylase (HDAC) Inhibitor Trichostatin A (TSA) wurden als Substanzen in den Experimenten eingesetzt, weil vorhergehende Versuche bereits auf mögliche antikanzerogene Effekte hindeuteten. Zunächst wurden verschiedene Transfektionsmethoden ausgetestet, damit in der Folge ein Gen Reporterassay durchgeführt werden konnte. Dabei wurde das neue K2®Reagenz als effektivste Transfektionsmethode identifiziert, welches auch die Transfektion der hoch transfektionsresistenten Neuroblastom Zellen erlaubte. Daraufhin wurde die Amplifikation von MYCN in Kelly und IMR-32 Zellen im Vergleich zu SH-SY5Y Zellen sowohl auf mRNA Ebene als auch auf Proteinebene bestätigt. Die hohe Empfindlichkeit der SH-SY5Y Zellen gegen Simvastatin konnte bestätigt werden, während die Viabilität der beiden MYCN amplifizierten Zelllinien nicht von dieser Substanz beeinflusst wurde. Im Gegensatz dazu war es möglich mit VX680 die IMR-32 Zellen abzutöten und mit TAE684 konnte die Viabilität sogar in allen drei Zelllinien signifikant reduziert werden. Das erlaubt nun die Vermutung, dass der Anaplastische Lymphomkinase Signalweg wichtig für das Überleben in allen drei Zelllinien zu sein scheint. Neue Behandlungsmöglichkeiten könnten von dieser Entdeckung profitieren.

3 Abstract

Neuroblastoma is an unpredictable heterogeneous tumour for which MYCN amplification has been described as one of the rare consistent genetic markers that is correlated with unfavourable outcome for the patient. Various compounds are believed to participate in the process of N-Myc transcription factor stabilization leading to high concentrations in the cell. Therefore, they are considered promising targets for pharmacological intervention against this malignant disease.

The main goal of this study was to examine the effects of selected drugs on viability and apoptotic events in three primary human neuroblastoma cell lines. The not MYCN amplified SH-SY5Y cell line served as control cell line and was compared to Kelly and IMR-32 cell lines which are MYCN amplified. Furthermore drugs were applied in double combinations for identification of additional and possible synergistic effects. HMG-CoA reductase inhibitor simvastatin, aurora kinase A inhibitor VX680, anaplastic lymphoma kinase (ALK) inhibitor TAE684 and histone deacetylase (HDAC) inhibitor trichostatin A (TSA) were applied as substances in the experiments because previous experiments already suggested possible anti-cancer effects. First, in order to be able to conduct gene reporter assays various transfection methods were performed to identify the most effective agent, which turned out to be the new K2®reagent. This agent is an effective new transfection reagent in highly transfection resistant neuroblastoma cells. Then, the amplification of MYCN in Kelly and IMR-32 cell lines was confirmed on RNA level as well as on protein level compared to SH-SY5Y cells. Most importantly, the high susceptibility of SH-SY5Y cells to simvastatin was confirmed while the viability of MYCN amplified cell lines was not affected by this drug. In contrast, VX680 was able to kill IMR-32 cells and TAE684 could significantly reduce viability in all three cell lines. This allows the suggestion that the anaplastic lymphoma kinase pathway seems to be important for the survival of all three cell lines. New possible treatment options could profit from this finding.

4　Abbreviations

°C	degree Celsius
µF	microfarad
µg	microgrammes
µl	microliters
µM	micromolar
Akt	protein kinase B
ALK	anaplastic lymphoma kinase
AT	Austria
BAFF-R	B-cell activating factor receptor
Bcl-2	B-cell lymphoma 2 protein
BDNF	brain derived neurotrophin factor
bHLHZ	basic helix-loop-helix leucine zipper domain
Bp	base pairs
BSA	bovine serum albumin
$CaCl_2$	calcium chloride
Cdk1	cyclin dependent kinase 1
CH	Switzerland
cl.	cleaved
CRI	cancer related inflammation
CTL	control
DE	Germany
DMSO	dimethylsulfoxide
DNA	desoxyribonucleic acid
dNTPs	desoxynucleosidtriphosphates
DR	death receptors

E-box	enhancer box
ECL	enhanced chemoluminescence
EDTA	ethylenediaminetetraacetic acid
eGFP	enhanced green fluorescent protein
FACS	fluorescence activated cell sorting
FBS	fetal bovine serum
Fbxw7	F-box/WD repeat-containing protein 7
FDA	United States Food and Drug Administration
Fwd	forward
GAPDH	glycerinaldehyd-3-phosphat-dehydrogenase
Gsk3	glycogen synthase kinase 3
GTPase	guanosine triphosphatase
H_2O	water
HCl	hydrochloric acid
HDAC	histone deacetylase
HEPES	2-(4-(2-Hydroxyethyl)- 1-piperazinyl)-ethansulfon acid
HMG-CoA	3-hydroxy-3-methylglutaryl-coenzyme A
HRP	horse reddish peroxidase
HSCT	hematopoietic stem cell transplants
IDRF	image defined risk factors
IKK1	IκB kinase complex 1
IL-1β	interleukin-1β
INRGSS	International Neuroblastoma Risk Group Staging System
INSS	International Neuroblastoma Staging System
IκK	IκB kinase
JP	Japan
k/rpm	kilo/rounds per minute

KCl	potassium chloride
kDa	kilodalton
KH_2PO_4	potassium dihydrogenphosphate
LB medium	Luria Bertani medium
LPS	lipopolysaccharides
LTβR	lymphotoxin β receptor
Luci	luciferase
MAX	MYC-associated protein X
MBI, MBII, MBIII, MB IV	Myc box I, II, III, IV
mg	milligrams
MHCII	major histocompatibility complex II
MIBG	meta-iodobenzyl-guanidine
min	minutes
ml	millilitres
mm	millimetres
MQ	milli-Q
MTT	3-(4,5-dimethylthiazol-2-yl)-2,5-diphenyltetrazoliumbromide
MXD1	MYC/MAX/MAX dimerization protein 1
MYC	V-myelocytomatosis viral related oncogene homolog
MYCL	V-myelocytomatosis viral related oncogene, lung carcinoma derived homolog
MYCN	V-myelocytomatosis viral related oncogene, neuroblastoma derived (avian)
n.s.	not significant
Na	sodium
$Na_2HPO_4.2H_2O$	disodiumhydrogenphosphate dehydrate
NaCl	sodium chloride
$NaHCO_3$	sodiumhydrocarbonate

NaN$_3$	sodium azide
NB	neuroblastoma
NFκB	nuclear factor binding the κ light chain of activated B cells
ng	nanogrammes
NGF	neurotrophin nerve growth factor
NIK	NFκB inducing kinase
nm	nanometers
nM	nanomolar
PARP-1	poly ADP ribose polymerase 1
PBS	Potassium Buffered Saline
PCD	programmed cell death
PCR	polymerase chain reaction
PHOX2B	paired-like homeobox 2b
PI3 kinase	phosphoinositide-3 kinase
RANK	receptor activator of NFκB
Ren	renilla
Rev	reverse
RNA	ribonucleic acid
SD	standard deviation
SDS-PAGE	sodiumdodecylsulfate-polyacrylamide gel electrophoresis
sec	seconds
Sim	simvastatin
SIOPEN	Society of Pediatric Oncology Europe Neuroblastoma Group
TAE	Tris EDTA buffer
TAE buffer	Tris acetate EDTA buffer
TBS	Tris Buffered Saline
TBST	Tris Buffered Saline with Tween 20

TEMED	tetramethylethylendiamin
TNFSFRs	tumour necrosis factor superfamily receptors
TNFα	tumour necrosis factor α
TRAIL	TNF-related apoptosis-inducing ligand
Tris	Tris(hydroxymehyl)aminomethane
TrkA, TrkB	tropomyosin receptor kinase A, B
TSA	trichostatin A
UK	United Kingdom
USA	United States of America
V	Volt
w/o	without

5 Introduction

5.1 Neuroblastoma - A highly various childhood tumour

Being the third most common childhood malignancy after leukaemia and brain tumours, this extra-cranial solid tumour derives from neural crest cells, primitive cells of the sympathetic nervous system, and appears in children from 0-14 years.[1-3]

Neuroblastoma (NB) is an unpredictable heterogeneous tumour which can on the one hand result in severe metastatic disease or differentiate to ganglioneuroblastoma and ganglioneuroma.[4] But on the other hand, there are also a notable number of tumours that can undergo spontaneous regression even without any treatment.

Symptoms of the disease, however, depend on the location of the primary tumour along the sympathetic nervous system and on the presence of metastases (Figure 1). Most common is an intra-abdominal primary tumour often regarding the adrenal gland region.[5] Periorbital involvement also referred to as "Hutchison's syndrome" can lead to ecchymoses and blindness. "Horner's syndrome" is a symptom resulting from upper chest tumours that intercept the sympathetic chain. Metastatic disease can also lead to bone and bone marrow as well as liver and skin involvement.
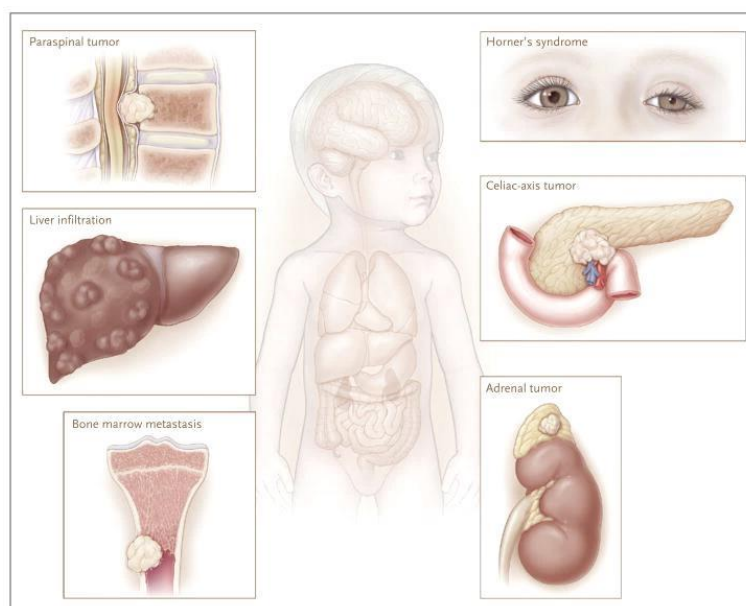
Figure 1: Symptoms of Neuroblastoma depend on tumour locations. (Maris, 2010)[6]
Primary tumours often concern adrenal glands and metastatic developments can lead to liver, spine, bone marrow and periorbital involvement

5.1.1 Staging Systems

NB may be one of the most common diseases in children but still there are only a small number of patients.[5] Therefore, for a long time a variety of clinical and biological data were used in different regions all over the world in order to decide over treatment options and prognosis for the individual patient. Establishing a consistent risk stratification system was the first step towards comparable clinical trials and stage appropriate treatments.

Nevertheless, due to the heterogeneity of this tumour defining stratification stages was a great challenge. The first big step was the International Neuroblastoma Staging System (INSS) which was developed in 1986 and published by Brodeur *et al.* in the Journal of Clinical Oncology (Figure 2).[7] But as staging of patients with the INSS requires resection of the tumour it is among others also depending on operative findings and thus on the surgeon's performance and experience.[5,8] Therefore, an even more accurate system has been established recently which allows to determine "image-defined risk factors (IDRFs)" by pre-operative radiographic tumour imaging. These IDRFs were already established by the International Society of Pediatric Oncology Europe Neuroblastoma Group (SIOPEN) in 1994.

They were adopted and further used to stage the disease together with INSS criteria. The International Neuroblastoma Risk Group Staging System (INRGSS) used these factors and analysed 8800 patients to define 4 different stages of the disease (Figure 3).

Stage	Definition
1	Localized tumor with complete gross excision, with or without microscopic disease; representative ipsilateral lymph nodes negative for tumor microscopically (nodes attached to and removed with the primary tumor may be positive).
2A	Localized tumor with incomplete gross excision; representative ipsilateral non-adherent lymph nodes negative for tumor microscopically.
2B	Localized tumor with or without complete gross excision; representative ipsilateral non-adherent lymph nodes positive for tumor. Enlarged contralateral lymph nodes must be negative microscopically.
3	Unresectable unilateral tumor infiltrating across the midline, with or without regional lymph node involvement; or midline tumor with bilateral extension by infiltration (unresectable) or by lymph node involvement. *Midline is defined as vertebral column.*
4	Any primary tumor with dissemination to distant lymph nodes, bone, bone marrow, liver, skin and/or other organs (except as defined for stage 4S).
4S	Localized primary tumor (as defined for stage 1, 2A or 2B), with dissemination limited to skin, liver and/or bone marrow (limited to infants, 1 year of age). *Bone marrow involvement < 10%.*

Stage	Definition
L	Localized tumor not involving vital structures as defined by the list of image-defined risk factors and confined to one body compartment.
L2	Locoregional tumor with presence of one or more image-defined risk factors.
M	Distant metastatic disease (except stage MS).
MS	Metastatic disease in children younger than 18 months with metastases confined to skin, liver, and/or bone marrow.

Figure 2: Brodeur *et al.* published the International Neuroblastoma Staging System (INSS) in 1988 (Owens and Irwin, 2012)[5]

Figure 3: The International Risk Group Staging System (INRGSS) (Owens and Irwin, 2012)[5]

5.1.2   Diagnosis and risk factors - A molecular and genetic insight

In addition the INRGSS biological and genetic factors can be considered for diagnosis and thus facilitate an accurate treatment and prognosis.

Although most of the time somatic changes are responsible for NB to arise, in about 1-2% of the cases the disease can also be inherited.[7,9] Mutations in ALK and PHOX2B were proven to be involved in pre-dispositional NB. But nevertheless most of the time tumours develop spontaneously.

Brodeur *et al.* proposed a model for NB development according to different genetic features being correlated with favourable or unfavourable outcome.[9,10] It divides NB into two general types arising from a single common precursor (Figure 4).
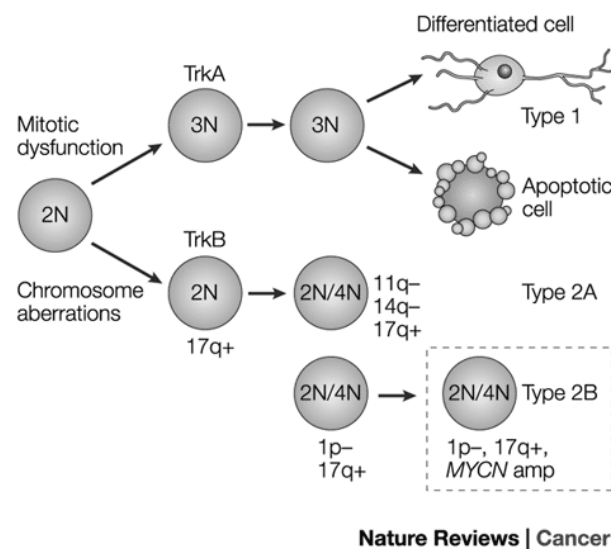
Figure 4: Genetic development of NB can be divided into 2 subsets. (Brodeur, 2003)[10]
Type 1 leads to a favourable outcome because of cell differentiation or apoptosis due to near-triploid karyotype and high TrkA expression. Type 2 NB present with near-diploid or -tetraploid state with gain of 17q. Type 2A involves loss of 11q and/or 14q while type 2B often shows MYCN amplification and loss of 1p heterozygosity.

Type 1 NB develops a near-triploid state with whole chromosome gains after mitotic malfunction. And because of high expression of TrkA neurotrophin receptor cells differentiate or enter apoptosis depending on presence or absence of its ligand, neurotrophin nerve growth factor (NGF).[11] High TrkA expression has also been exposed to be part of the mechanism due to which NB can spontaneously regress.[9] This type of tumour is generally detected at a young age and prognosis for patients is good.[10] Conversely, type 2 NB presents a near-diploid or near-tetraploid state and involves chromosome aberrations leading to 17q gain. Also a high expression of neurotrophin receptor TrkB plus ligand, brain derived neurotrophin factor (BDNF), is typical for this type of NB. Type 2 NB can furthermore be divided into two subtypes. Type 2A shows no MYCN amplification and loss of 11q and/or 14q. These children usually suffer from more advanced stages of the disease with

unfavourable outcome. Type 2B, however, being the most aggressive species usually involves MYCN amplification and loss of chromosome 1p heterozygosity. All in all, the MYCN proto-oncogene was found to be amplified in about 22% of primary tumours being one of the rare genetic factors consistently associated with poor prognosis.[12]

In the end, age and stage of disease at diagnosis are most crucial for the survival of the patient. This is the reason why scientists in different countries decided to screen new-borns for elevated levels of catecholamines and their metabolites in urine, allowing rapid diagnosis without invasive testing.[5,8] Over 90% of NB secrete epinephrine and dopamine which leads to elimination of their metabolites homovanillic acid and vanillylmandelic acid in urine.[5] But these screening processes did not turn out to be very constructive as they only led to identification of more children suffering from NB while the mortality rates did not change. This leads to the assumption that most of the additionally diagnosed tumours would probably have regressed without any treatment anyways.

5.1.3   Common treatment options and possible new approaches

As explained already this paediatric disease is very heterogeneous and a lot of therapy options are available. Usually multimodality treatment is applied to more aggressive types of NB.[2] Therefore, in order to minimize sequelae and avoid overtreatments patients must be divided into low risk, intermediate and high risk classes and treatments must then be chosen accordingly.[2,5] Tumours in low risk patients with stage L1 in according with the INRGSS are surgically resected or frequently they are only observed. At this stage the disease is survived by more than 90% of patients even with minimal therapy.[13] Patients with stage L2 NB are considered at intermediate risk and surgery is often complemented with pre-operative chemotherapy administrating for example doxorubicin, cisplatin, cyclophosphamide or teniposide.[2,14] Still the bigger part of patients with stage L2 NB expects a positive outcome. For high risk patients with stage M/MS multimodality treatments come into use. Chemotherapy and surgery are applied together with radiation therapy. Patients can furthermore be treated with hematopoietic stem cell transplants (HSCT) and immunotherapy. But still in about every second child with M/MS stage the disease will relapse.[15]

The low survival rate of patients with higher stages of the disease and the aftermath for children treated with aggressive cytotoxic agents and radiation is the motivation to look for more selective treatments. Therefore, newer approaches try to consider more thoroughly the biology and pathways of tumour formation as well as the unique tumour regression in NB.[9,10]

Treatments with retinoic-acid derivatives led to good results in clinical trials.[16,17] They were proven to drive NB cells into differentiation and seem to be associated with higher Trk B receptor expression.[9] Therefore they have become a standard treatment for patients with high risk NB after bone marrow or stem cell transplantation.[10] Another approach leading to cell differentiation is the administration of histone deacetylase (HDAC) inhibitors such as Vorinostat.[9,18] Although HDAC inhibitors have led to diverse results in studies so far the better knowledge of epigenetic features in NB could be crucial for identifying an effective treatment. Furthermore the induction of apoptotic events in cancer cells is of course a promising approach. Several agents are in trials, for example Trk specific tyrosine kinase inhibitors were proven to be effective in xenografts.[19] Conventional radiation therapy not only harms tumour cells but also non-transformed cells of the body.[10] Targeted radiation therapy reduces these side effects efficiently. Radioactive meta-iodobenzyl-guanidine (MIBG) is applied for this purpose as NB cells tend to take up this tracer.[20] Especially applied before surgery this method can help to reduce tumour size and thus allows a more efficient resection. Immunotherapy also uses the principle of targeted therapy aiming to avoid damages to the rest of the system. But to be able to conduct therapeutic agents directly to cancer cells one has to know the according antigens.[21] The ideal immune targets would be antigens expressed on tumour cells only and not being present in other tissues. As these ideal antigens have not yet been detected for NB this is still an important goal of current investigations. Experiments with immunomodulatory cytokines even led to the assumption that host-mediated immune responses are able to induce spontaneous tumour regression.[9] This research is therefore of utmost interest. Further promising concepts specifically concern mutations with oncogenic potential in drug-resistant and refractory NB such as the human anaplastic lymphoma kinase (ALK) and aurora kinase A. ALK gene is a down-stream target of N-Myc and has also been found to be upregulated and involved with cell migration and invasion in NB with unfavourable outcome.[22] One of the first ALK inhibitors tested was the

NVP-TAE684.[23] Although this compound never entered clinical trials further ALK inhibitors were developed and crizotinib by Pfizer was finally FDA approved.[24] But research is continuing on this field and newer inhibitors even show better affinities to ALK and promising treatment results. Another meaningful target for drug therapy seem to be aurora kinases.[25] Aurora kinases were discovered being involved in cancer development in 1995 and since then they became of great interest as drug targets. In NB especially aurora kinase A signalling is relevant.[26] Aurora A expression or amplification also serves as negative prognostic feature and was furthermore identified to play an important role in inhibiting N-Myc protein degradation in MYCN amplified NB cells.[27] Thus, cells are kept in cell cycle and in proliferative state leading to cancer evolution. Tozasertib (VX680), a pan aurora kinase inhibitor, and the second generation inhibitor, alisertib, demonstrated the potential of these new targets in cell culture trials.[25]

5.2 Myc - Family of proto-oncogenes

In 1979 Roussel *et al.* discovered the viral oncogene c-MYC carried by the avian acute leukaemia virus MC29 in myelocytomatosis.[28]

Soon after in the 1980ies the role of c-MYC and paralogs in tumourigenesis was uncovered. Amplification of c-MYC was linked to the development of myeloid leukaemia and colon carcinomas.[29,30] Schwab *et al.* published in 1983 that MYCN is amplified in NB and furthermore that amplification was correlated with poor outcome for these patients.[31] The third vertebrate MYC family member, MYCL1, was discovered to be amplified in small cell lung carcinomas.[32]

5.2.1 Myc protein organization

C-Myc (c-MYC), N-Myc (MYCN) and L-Myc (MYCL1) were all found to be located in the nucleus and to be involved in gene regulation.[33] The proteins contain three regions that are built similarly in all of the three family members. The N-terminal region containing the conserved MYC-boxes MBI and MBII is important for transcriptional activation. The centre region includes two additional conserved MYC boxes, MBIII and MBIV, and proline, glutamic acid, threonine and proline residues are predominate. The C-terminal region consists of the basic helix-loop-helix leucine zipper domain (bHLHZ). This bHLHZ region is known to mediate dimerization.[33,34] However MYC proteins typically do not form homodimers but interact specifically with MYC-associated protein X (MAX). These dimers then bind to consensus E-box promoter sequences on DNA (5'-CACGTG-3') via their basic region and thus stimulate transcription of genes involved in differentiation and proliferation. The omnipresent MAX protein also forms heterodimers with MYC/MAX/MAX dimerization protein 1 (MXD1).[34] Interestingly, these MAXD1-MAX heterodimers can interact with the same E-box recognition sites as MYC-MAX dimers but repress transcription of those genes. Therefore, MAX is important for both the activation and negative regulation of transcription. Nevertheless, it has been established that MYC has several additional functions alone and in absence of MAX and furthermore MYC can interact with other proteins than MAX that also bind to DNA promoter regions.[33,35]

5.2.2 MYC protein functions and their role in cancer formation

The role of MYC associated with cancer is not surprising as it is involved in pathways crucial for cell cycle and growth, proliferation, differentiation and pluripotency.[36] There are lots of products of various signal-transduction pathways that end up activating MYC transcription (Figure 5) and in healthy cells the transcription of MYC genes and mRNA stabilities as well as MYC translational events and MYC protein stabilities are very tightly regulated.[33] But in cancerous development these regulations are somehow disturbed and MYC levels are elevated.

For example, MYC proteins are normally very unstable and have half-lives of only 15-20 minutes.[37] First, their transcriptional functions are initiated by phosphorylation at MBI and after the proteins have fulfilled their purpose they are ubiquitinylated at MBI and degraded.[33,38] One way by which MYC protein concentrations are elevated in cancerous cells is the stabilization of the protein by mutations at the ubiquitin ligase binding sites. And in many cancer types such as NB MYC genes were found to be amplified and therefore MYC expression is higher.[31]

While MBI is important for degradation processes of MYC, MBII is the central spot for binding of different crucial interactors such as members of histone acetyltransferase (HAT) complexes.[33] By acetylation of histones genes can be activated.

MYC's main function is of course the regulation of transcriptional events being among others directly part of the transcriptional process with RNA polymerase I and III.[33,38] But not does MYC only activate gene transcription it is also involved in gene repression, for example by activating microRNAs.

Nevertheless, MYC has also other functions in non-transcriptional events. It was proven to stimulate DNA replication.[39] Furthermore, MYC can be cleaved in cytoplasm and the MYC fragment "MYC-Nick" is then involved in differentiation processes.[40]
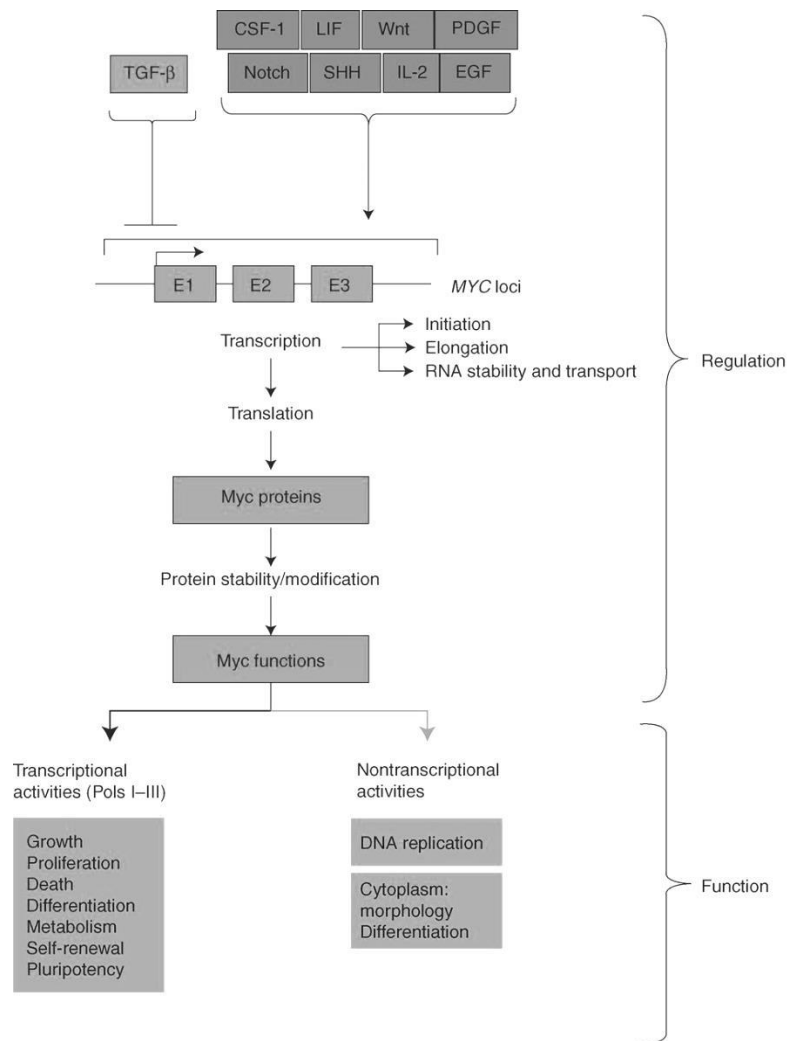
Figure 5: MYC regulation and functions. (Conacci-Sorrell *et al.*)[33]
Many products of various signal-transduction pathways activate MYC transcription and the protein expression
is very tightly regulated, too. MYC functions are highly variable and it does not only have functions in
transcription but also in DNA replication and differentiation.

All in all, high-throughput methods revealed MYC being bound to about 15% of promoters in
the genome.[41,42] But it does not influence the expression of all those genes. So the common
theory is that MYC needs additional factors to be able to act as a transcription factor and
that those factors (histone acetylases, methyltransferases, basal transcription factors etc.)
are in the end responsible for MYC's final functions, activation or repression.

Furthermore, it was found that there are E-box regions that are usually occupied by other
transcription factors in homeostasis.[38] And when cells switch to the proliferative state, due
to the elevated MYC levels, it can promiscuously interact with those same E-boxes. The

constant high MYC levels in cells with genetic or molecular malfunctions in its normally tightly regulated pathway could explain the formation of cancer, because cells are kept under constant proliferation.

5.2.3 N-Myc in neuroblastoma and therapeutic opportunities

As mentioned already, in NB amplified MYCN is correlated with advanced stages and with poor prognosis for patients and furthermore tumours that develop after the influence of Myc stay also Myc dependent.[10,27,31] Therefore, an interesting question is how one could intervene with targets up-stream or down-stream of N-MYC.

One kinase identified to be crucial for N-MYC stability is aurora A because it protects the protein of degradation by formation of a complex.[27,43] During G2 phase of cell cycle and mitosis N-Myc in neuroblasts is first phosphorylated by cyclin B/Cdk1 and Gsk3 and then degraded by Fbxw7 after ubiquitination (Figure 6).[27,44] Subsequently cells can exit cell cycle as proliferation is no longer mediated by N-Myc. Cells start to mature and differentiate. On the other hand, Gsk3 can be blocked by phosphorylation via Akt. This together with PI3-kinase signalling leads to a stabilization of N-Myc protein and cells are kept in proliferative state. PI3 kinase inhibition did not lead to the expected effect of lowering N-MYC protein concentrations but in the course of those experiments it was proven that high aurora A levels were responsible for this contradictory event.[27] High aurora A concentrations are able to protect phosphorylated N-Myc from degradation and therefore they seem to be another factor responsible for the formation of NB. A positive feedback loop exists between amplified MYCN that leads to high expression of aurora A and high aurora A levels on the other hand that inhibit N-Myc degradation.
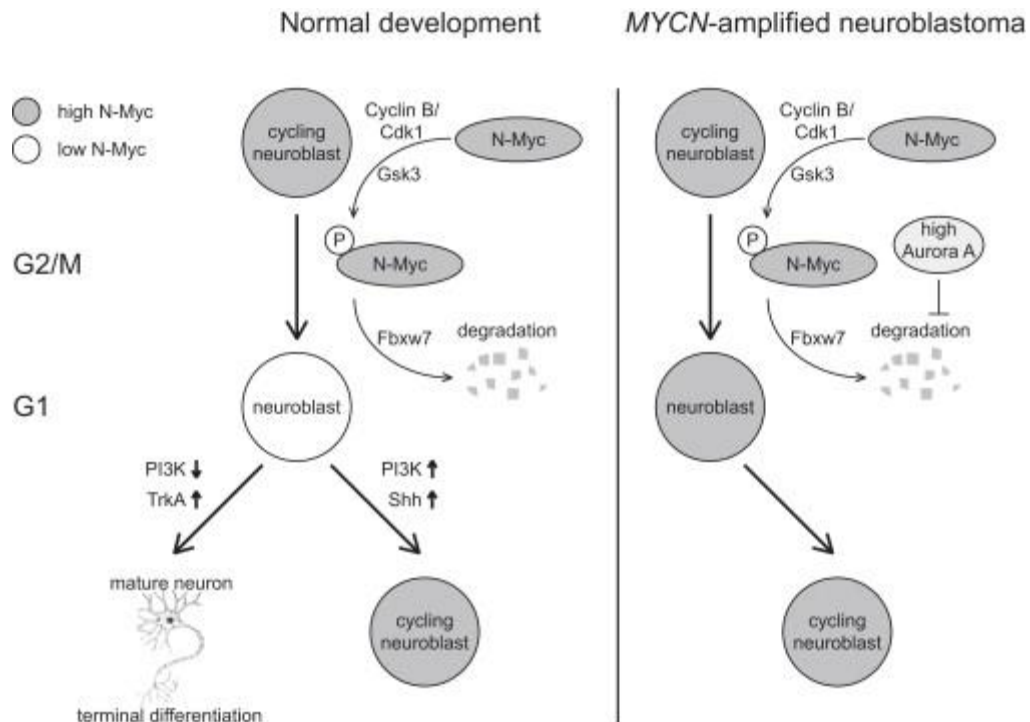
Figure 6: Normal development of neuroblasts vs. development of MYCN amplified neuroblasts. (Otto et al., 2009)[27]

In normal development cycling neuroblasts have high N-Myc levels but during G2 phase and mitosis N-Myc is phosphorylated and subsequently degraded. Therefore cells do not longer get the signals to proliferate and exit cell cycle and differentiate. In MYCN amplified cells high N-Myc levels keep cells in cell cycle. A positive feedback loop exists between amplified MYCN and high expression of aurora a and high levels of aurora A stabilizing the N-Myc protein

5.3 Statins and their pleiotropic effects

Mevalonate is the precursor for isoprenoids like farnesyl pyrophosphate and geranylgeranyl pyrophosphate (Figure 7).[45,46] The final product of the mevalonate pathway is cholesterol. It is synthesized by a precisely regulated reaction the rate limiting enzyme being 3-hydroxy-3-methylglutaryl Coenzyme A (HMG-CoA) reductase.[45,47]

Isoprenoids play an important role in posttranslational modifications of proteins (prenylations).[46,48] Prenylation anchors the targeted proteins, e.g. the small guanosine triphosphatases, GTPases (Ras, Rho, Rac), to the cell membrane. When isoprenoid synthesis is inhibited signal transduction pathways are disturbed with profound influence on cell proliferation and differentiation, which often leads to apoptosis.
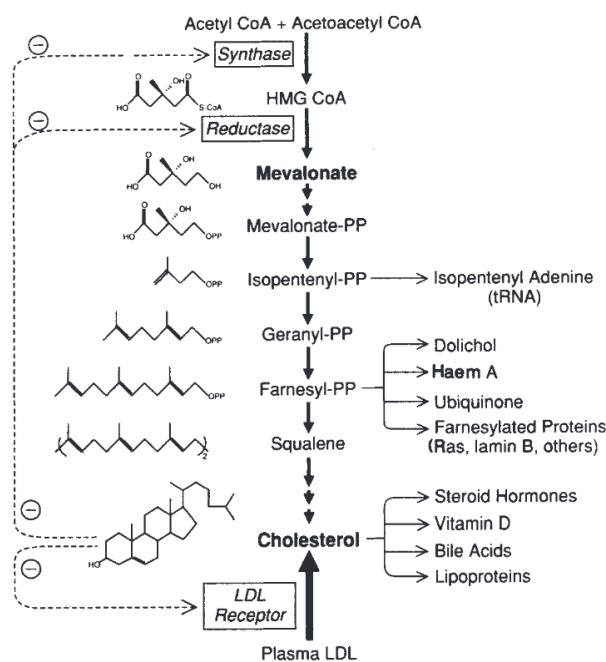
Figure 7: Regulation of mevalonate pathway in animals. (Goldstein and Brown, 1990)[45]
Mevalonate is synthesized from acetyl-CoA and acetoacetyl-CoA in a reaction catalysed by the HMG-CoA synthase and reductase. The bulk product of the pathway is cholesterol.

HMG-CoA reductase competitive inhibitors called statins were found to be effective against the health problems caused by hypercholesterolemia due to their lipid-lowering effects.[48]

Therefore, statins are nowadays commonly prescribed against cardiovascular diseases also prophylactically.[49] Since their discovery many different statins have been detected and developed and one can distinguish between statins of natural origin like simvastatin or lovastatin and synthetic statins like fluvastatin, rosuvastain, pitavastatin or atorvastatin.[46] Besides their cholesterol-lowering effects statins are known for their pleiotropic impacts.[48,49] One of these versatile effects is the immunomodulation by statins.[48,50] Statins were shown to repress interferon γ and thus inhibit the major histocompatibility complex class II (MHC-II) dependent T-cell activation. Moreover, statins are involved in stimulation of leukocyte migration and influence on cytokines. A statin therapy could therefore not only help patients to suppress the immune system after transplantation surgery but furthermore it could be applied against other diseases involving the immune system like for example diabetes type I. Different studies also proved the anti-inflammatory effects of statins.[48] Their inhibition of cytokines that induce inflammation like interferon γ, tumour necrosis factor α and interleukins was shown in different cell types. Furthermore, angiogenesis and protection of endothelial cells is influenced by statin therapy which has been shown in several animal models and can also be inferred from clinical trials with hypercholesterolemia patients.[51,52] While higher doses can inhibit angiogenesis lower statin concentrations seem to have the opposite effect.[48] Angiogenesis plays a crucial role in cancer development, in atherosclerosis, diabetic retinopathy and further illnesses and therefore statins could reveal new possible treatment options.

Nevertheless, one of the most promising is the apparent anti-tumour effect of statins which comes along with the above mentioned properties.[48] That is why statins have been discussed as possible chemoprevention drugs.[53] As mentioned above different mevalonate pathway derivatives are necessary for several cell functions such as prenylation. Disturbances in their synthetic pathways can affect protein functions and thus lower tumour growth and induce apoptotic events.[51,54,55] Furthermore, the inhibition of angiogenesis and cell migration impairs metastatic events. But one has to mention that these effects were found to differ highly among different cell types and with different drug concentrations.[48] Also the results of different studies are often contradictory.[53,54]

5.4   NFκB – A link between inflammation and cancer

The nuclear factor NFκB got its name because it was discovered binding to an enhancer region of the immunoglobulin κ light-chain of activated B cells.[56,57] But further examination revealed the much more versatile functions of NFκB. Altogether the NFκB family comprises five homologous transcription factors that share the highly conserved Rel domain which is significant for DNA-interaction as well as dimerization.[56,58] The proteins can be grouped into two different classes.[58] The first class includes the proteins p105 and p100. These two transcription factors are inhibited by ankyrin repeats in their own C-terminus and are only activated by being cleaved into smaller proteins, p50 and p52.[56] They do not possess a transactivation domain and therefore dimers of these proteins binding to the according promoter regions repress transcription. When bound to members of the second class of protein family however, they become transcriptional activators. The second class of NFκB transcription factors consists of c-Rel, RelA (p65) and RelB. They contain transactivation domains in their C-terminus and bind to gene promoters after dimerization. Those proteins are usually bound to IκB inhibitors which contain ankyrin repeats and therefore repress their transcriptional activity. All in all, the NFκB signalling pathway is very complex as the proteins form different dimers, bind to a variety of genes, their activation is influenced by a number of post-translational modifications such as phosphorylation and furthermore they interact with lots of other proteins.[56,58,59]

Basically, two different NFκB signalling pathways can be distinguished (Figure 8).[57] The canonical pathway is initiated when cytokines like tumour necrosis factor α (TNFα) and interleukin-1 β (IL-1β) or antigens like lipopolysaccharides of bacterial cell walls (LPS) bind to tumour necrosis factor receptor, Interleukin-1 receptor or antigen receptors.[56,57] This causes the IκB kinase complex (IKK) to phosphorylate IκB proteins bound to NFκB proteins. Thus, ubiquitination of the inhibitory protein can occur which is followed by proteasome degradation and the transcription factor can be transferred into the nucleus.[56,57,60] The non-canonical pathway on the other hand is triggered by binding of a subset of the tumour necrosis factor superfamily receptors (TNFSFRs), like B-cell activating factor receptor (BAFF-R), CD40, receptor activator of NFκB (RANK) and lymphotoxin β receptor (LTβR).[56,59] Then the NFκB inducing kinase (NIK) phosphorylates IKK1. This leads to phosphorylation of

p100 allowing its ubiquitination and cleavage into the active p52 followed by transfer into the nucleus to fulfil the transcription activating purpose. Furthermore, some atypical NFκB activation pathways have been described.
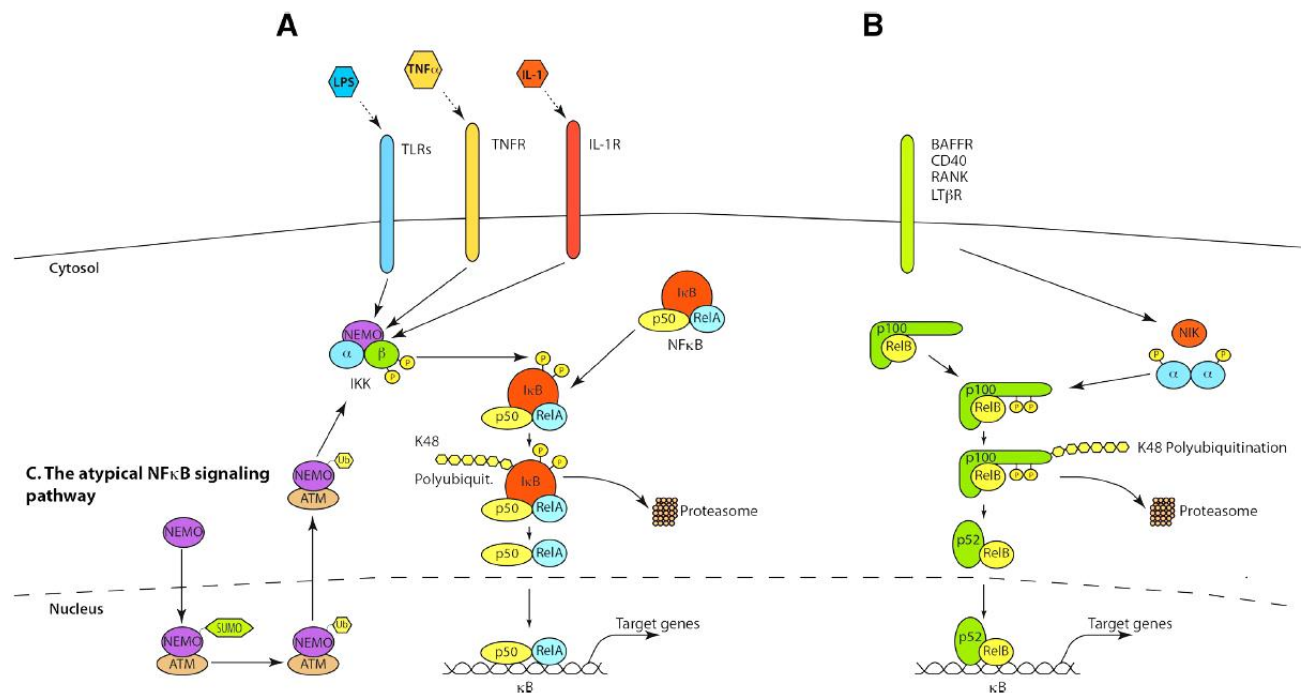
Figure 8: NFκB signalling pathways (Hoesel and Schmid, 2013)[56]
The canonical pathway is initiated by binding of TNFα, LPS or IL-1 (A) and the non-canonical pathway is activated by binding of BAFFR, CD40, RANK or LTβR (B). Furthermore there exists an atypical pathway (C).

As immune and inflammatory cells infiltrate solid tumours, cancer-related inflammation (CRI) is referred to as one of the hallmarks of cancer.[58,61] The transcription factor NFκB was detected as crucial factor regarding the involvement of inflammation in cancer development. Nevertheless, NFκB can have ambiguous roles regarding cancer.[56] For instance, in acute inflammation it has a key role in the immune defence attacking transformed cells and leading to the activation of cytotoxic cells of the immune system. If constitutively active, however, it was also found to have a cancer supporting role. Constitutively high NFκB activities in tumours can be triggered by intrinsic factors such as genetic alterations or extrinsic factors like an elevated cytokine production from the tumour

microenvironment.[56,61,62] NFκB in tumours leads to pro-survival effects of the cells by up-regulation of the according genes, to an elevated immune response and to the recruitment of leukocytes.[56] Some of the most prominent examples where inflammation is associated with cancer are colon cancer, hepatocellular cancer, melanoma and also lung cancer.

5.5 Apoptosis signalling pathways - Targets for cancer therapy

Two ways of cell death can be told apart: necrosis and programmed cell death referred to as apoptosis.[63] While necrosis leads to inflammatory reactions apoptotic cells in the body are immediately removed by phagocytosis. Mutations that make tumour cells resistant to programmed cell death (PCD) are considered another hallmark of cancer besides CRI.[64] Survival of these mutated defective cells can lead not only to cancer formation but also to a variety of other diseases.

Basically, two different pathways of apoptosis signalling can be distinguished in mammals.[65] Both of these pathways activate a complex cysteine protease cascade leading to morphological and biochemical changes in the cell. Caspases are grouped into upstream initiator caspases (caspase-8, -9, -10) and downstream effector caspases (caspase-3, -6, -7) which are activated by the upstream caspases.[63,66] The extrinsic apoptosis pathway is initiated by extracellular death ligands interacting with the appropriate death receptors (DR).[64-67] Death ligands such as FasL and TNF-related apoptosis-inducing ligand (TRAIL) are released from immune cells. Procaspase 8 is cleaved before activating down-stream effector Caspase 3. In this case mitochondria are not involved in the apoptosis signalling pathway. The intrinsic pathway, on the other hand, involves intracellular signals initiating a mitochondrial apoptosis amplification loop. Members of the Bcl-2 family lead to the release of cytochrome c from mitochondria into the cytosol. Procaspase 9 is cleaved into caspase 9 leading among others to the cleavage and activation of Caspase 3.

Death ligands, especially TRAIL, are of great interest in drug trials regarding possible new cancer therapies targeting apoptosis pathways in tumour cells.[64] Moreover, TRIAL DR agonists show good results when combined with anticancer drugs such as doxorubicin and carboplatin as well as HDAC inhibitors.[65] Another approach is to address caspases and their substrates for activating the apoptosis pathway in cancer. For example, the caspase substrate Poly ADP ribose polymerase-1 (PARP-1) responsible for repair of damaged DNA and a crucial mechanism for cancer cells to develop drug resistance can be inactivated by gene inhibition or deletion.[64]

6 Aims

The aims of this project were…

- to evaluate N-Myc status of three different human neuroblastoma cell lines,

- to establish a non-viral transfection method for gene transfer in highly transfection resistant NB cell lines

- to identify drug targets and possible synergy in blocking various signalling pathways of NB cell lines

7 Material

7.1 Cell culture

Cell lines		
IMR-32	Human neuroblastoma cell line	Kindly provided by Children Cancer Research Institute; Wien, AT
Kelly	Human neuroblastoma cell line	Kindly provided by Children Cancer Research Institute; Wien, AT
SH-SY5Y	Human neuroblastoma cell line	Kindly provided by Children Cancer Research Institute; Wien, AT

Growth media		
RPMI-1640 Medium	With L-Glutamine and $NaHCO_3$; sterile filtered, liquid	R8758; Sigma Aldrich; Missouri, USA
Dulbecco's Modified Eagle's Medium	With 4500 mg glucose/L, L-Glutamine, $NaHCO_3$ and Pyridoxine.HCl; sterile filtered, liquid	D5796; Sigma Aldrich; Missouri, USA
Ham's Nutrient Mixture F12	With 1 mM L-Glutamine, sterile, liquid	51651C; Sigma Aldrich; Missouri, USA

7.2 PCR-Primers

PCR-Primers

GAPDH human fwd	41-4442-1/20; VBC Biotech; Wien, AT
GAPDH human rev	41-4442-2/20; VBC Biotech; Wien, AT
MYCN human fwd	11-3463-7/18; Eurofins MWG Operon Inc.; Alabama, USA
MYCN human rev	11-3463-8/18; Eurofins MWG Operon Inc.; Alabama, USA

7.3 Transformation – *E.coli* cells, restriction enzymes and buffers

E.coli cells

Competent XL 10_*Escherichia coli* cells	Kindly provided by Oliver Kudlacek

Restriction endonucleases

HindIII	ER0501; Fermentas, Thermo Fisher Scientific Inc.; Massachusetts, USA
NdeI	ER0581; Fermentas, Thermo Fisher Scientific Inc.; Massachusetts, USA

NheI	ER0971; Fermentas, Thermo Fisher Scientific Inc.; Massachusetts, USA
ScaI	ER0431; Fermentas, Thermo Fisher Scientific Inc.; Massachusetts, USA
XbaI	ER0681; Fermentas, Thermo Fisher Scientific Inc.; Massachusetts, USA

Buffers

Buffer Tango™ with BSA	BY5; Fermentas, Thermo Fisher Scientific Inc.; Massachusetts, USA
10 x Buffer SdaI with BSA	B24; Fermentas, Thermo Fisher Scientific Inc.; Massachusetts, USA

Plasmids

pEGFP-N1	Kindly provided by Oliver Kudlacek
pRL-TK	E2241; Promega; Wisconsin, USA
5x NFκB-luciferase	Kindly provided by Johannes Schmid

7.4 Transfection – Reagents and media

Transfection reagents

Fugene®6	E2691; Promega GmbH; Mannheim, DE
K2®Transfection System	T060-8.0; Biontex Laboratories GmbH; München, DE
TurboFect™	R0531; Thermo Fisher Scientific Inc.; Massachusetts, USA
Viafect™	E4983; Promega GmbH; Mannheim, DE
X-tremeGene 9	06366511001; Roche; Mannheim, DE
X-tremeGene HP	06365752001; Roche; Mannheim, DE

Medium for electroporation

Dulbecco's Modified Eagle's Medium	D5921; w/o L-glutamine and phenol red Sigma Aldrich; Missouri, USA

7.5 Drugs

Drugs

simvastatin	CAYM710010344-50; VWR International GmbH; Wien, AT
TAE684	S7062, (NVP-TAE684); Selleckchem; München, DE
TNFα	9511510; Strathmann Biotec AG; Hamburg, DE
Trichostatin A	L101142; Eubio; Wien, AT
VX680	S1048, Tozasertib (MK-0457); Selleckchem; München, DE

7.6 Antibodies

Primary antibodies

Anti-Caspase 3	9662; Cell Signaling; Cambridge, UK	Polyclonal antibody; 17/19/35 kDa, rabbit
Anti-NFκB p65	8242; Cell Signaling; Cambridge, UK	Monoclonal antibody; 65 kDa, rabbit
Anti-N-myc	9405; Cell Signaling; Cambridge, UK	Polyclonal antibody; 62 kDa, Rabbit
Anti-PARP	9542; Cell Signaling; Cambridge, UK	Polyclonal antibody; 16/89/24 kDa, rabbit
Anti-p-NFκB p65	3033; Cell Signaling; Cambridge, UK	Monoclonal antibody; 65 kDa, rabbit

Anti-p-STAT3 (Tyr705)	9131; Cell Signaling; Cambridge, UK	Polyclonal antibody; 79/86 kDa, rabbit
Anti-STAT3	9132; Cell Signaling; Cambridge, UK	Polyclonal antibody; 79/86 kDa, Rabbit
Anti-α-Tubulin	T6074; Sigma Aldrich; Missouri, USA	Monoclonal antibody; 50 kDa, mouse
Anti-β-Actin	A4700; Sigma Aldrich; Missouri, USA	Monoclonal antibody; 42 kDa, mouse

Secondary antibodies

| Anti-Mouse | 7076; Cell Signaling; Cambridge, UK | IgG HRP-linked antibody; goat |
| Anti-Rabbit | 7074; Cell Signaling; Cambridge, UK | IgG HRP-linked antibody; goat |

7.7 Kits

Kits	
Amersham™ECL™ Prime Western Blotting Detection Reagent	RPN2232; GE Healthcare; Buckinghamshire, UK
Deoxyribonuclease I	EN0521; Fermentas, Thermo Fisher Scientific Inc.; Massachusetts, USA
EZ4U Nonradioactive cell proliferation and cytotoxicity assay	BI-5000; Biomedica; Wien, AT
Firefly & Renilla Luciferase Assay Kit	30005-1; Biotium; Hayward, California, USA
HiSpeed® Plasmid Maxi Kit	12662; Qiagen AG; Basel, CH
RevertAid H Minus First Strand cDNA Synthesis Kit	K1632; Fermentas, Thermo Fisher Scientific Inc.; Massachusetts, USA
RNeasy® Mini Kit	74104; Qiagen AG; Basel, CH
Spectra™ Multicolor Broad Range Protein Ladder	26634; Thermo Fisher Scientific Inc.; Massachusetts, USA
SuperSignal®West Pico Chemiluminescent Substrate	34080; Thermo Fisher Scientific Inc.; Massachusetts, USA
peqGOLD Taq-DNA-Polymerase "all inclusive"	01-1000; PEQLAB Biotechnologie GmbH; Erlangen, DE

7.8 Other chemicals and acquired solutions

2-Mercaptoethanol	M-7154; Sigma Aldrich; Missouri, USA
6x DNA Loading Dye	R0611; Thermo Fisher Scientific Inc.; Massachusetts, USA
Acrylamide, N-N-methylenbisacrylamide	37.5:1; Fisher Scientific; Massachusetts, USA
Agar	05039; Fluka BioChemika, Sigma Aldrich; Missouri, USA
Ammonium Persulfate	9592.3; Roth; Karlsruhe, DE
Aprotinin	Trasylol®; Bayer; Leverkusen, DE
Bromphenolblue	B-5525; Sigma Aldrich; Missouri, USA
BSA	8076.4 Roth; Karlsruhe, DE
DMSO	4720.4; ROTIPURAN®; Roth; Karlsruhe, DE
DNA Ladder 1 kb GeneRuler™	SM0311; Thermo Fisher Scientific Inc.; Massachusetts, USA
DNA Ladder 1.000 bp	N0468G ; New England Biolabs GmbH; Massachusetts, USA
DNA Ladder 100 bp	N0467G ; New England Biolabs GmbH; Massachusetts, USA

EDTA.Na$_2$	8043.2; Roth; Karlsruhe, DE
FBS	F7524; Sigma Aldrich; Missouri, USA
Glycerol	4094; Merck; Darmstadt, DE
Glycerolphosphate	G6251; Sigma Aldrich; Missouri, USA
Glycin	3187.3; Roth; Karlsruhe, DE
HEPES	H3375; Sigma Aldrich; Missouri, USA
Hoechst Fluorescent Stain	33342; Thermo Fisher Scientific Inc.; Massachusetts, USA
Isopropanol	6752.1; ROTIPURAN®; Roth; Karlsruhe, DE
KCl	60132; Fluka BioChemika, Sigma Aldrich; Missouri, USA
KH$_2$PO$_4$	4873; Merck; Darmstadt, DE
Leupeptin Hemisulfate	CN33.2; Roth; Karlsruhe, DE
Methanol	8388.5; Roth; Karlsruhe, DE
Mowiol	475904; Calbiochem®; Merck Millipore; Darmstadt, DE

Na$_2$HPO$_4$.2 H$_2$O	71643; Fluka BioChemika, Sigma Aldrich; Missouri, USA
NaCl	3957.2; Roth; Karlsruhe, DE
NaN$_3$	438456; Sigma Aldrich; Missouri, USA
NP-40	74385; Fluka BioChemika, Sigma Aldrich; Missouri, USA
Paraformaldehyde	P6148; Sigma Aldrich; Missouri, USA
Pefablock	76307; Sigma Aldrich; Missouri, USA
Penicillin/Streptomycin	P11-010; PAA, GE Healthcare; Buckinghamshire, UK
Protein Assay Dye Reagent Concentrate	5000006; Bio-Rad Laboratories Inc.; California, USA
Serva DNA stain Green Clear G	39804.01; SERVA Electrophoresis GmbH; Heidelberg, DE
Sodium Dodecyl Sulfate	2326.2; Roth; Karlsruhe, DE
Tris	0188.1; Roth; Karlsruhe, DE
Triton X-100	93429; Fluka BioChemika, Sigma Aldrich; Missouri, USA
Trypan Blue	T8154; Sigma Aldrich; Missouri, USA

Trypsin-EDTA Solution (1x)	T3924; Sigma Aldrich; Missouri, USA
Tryptone Peptone	0123-17, Pancreatic Digest of Casein; Difco, Becton Dickinson; Maryland, USA
Tween 20	Tween® 20; Roth; Karlsruhe, DE
Yeast Extract	30701; Fluka BioChemika, Sigma Aldrich; Missouri, USA

8 Methods

8.1 Cell culture

8.1.1 Cell culture conditions

SH-SY5Y, Kelly and IMR-32 cells were cultured in T_{75} flasks in 13 ml of growth medium per flask. While SH-SY5Y cells were grown in a 1:1 mixture of DMEM and Ham's F12 medium, Kelly and IMR-32 cells were both grown in RPMI 1640 medium. 10% Fetal Bovine Serum (FBS) and 1% Penicillin/Streptomycin were added to both media. The cells were kept in the incubator at 5% CO_2 and 37°C.

8.1.2 Cell culture maintenance: Passaging cells

Cell medium was changed every 2-3 days and cells were split every 4-5 days after reaching about 80% confluence.

For detaching the adherent cells from the surface, first, they were washed with PBS (Table 1) and then treated with trypsin-EDTA and incubated for about 5 minutes at 37°C. Subsequently, the trypsin-EDTA solution was inactivated by adding the according growth medium to the cells.

The cell number was acquired by staining an aliquot of the cell suspension with Trypan Blue and counting the cells that had not absorbed the stain using a Bürker-Türk counting chamber. Thus, one obtains the number of vital cells per millilitre. Finally, cells were seeded in the required cell number. For example, in T_{75} flasks $1*10^6$ SH-SY5Y cells or $1.5*10^6$ Kelly or IMR-32 cells reach 80% confluence after 4-5 days.

PBS - Potassium Buffered Saline	
137 mM	NaCl
10,14 mM	Na_2HPO_4
2,7 mM	KCl
1,8 mM	KH_2PO_4
Diluted in MQ, pH adjusted to 7,4	

Table 1: Recipe for Potassium Buffered Saline (PBS)

8.1.3   Freezing and thawing cells

Cells were stored at -80°C in freezing medium (Table 2). After thawing the cells they were immediately diluted in growth medium and centrifuged (900 rpm, 5 minutes) to avoid toxic effects of the DMSO. The cell pellet was re-suspended in growth medium and cells were seeded in T_{75} flasks. The cells were cultured until reaching the passage number 25-30.

Freezing Medium
50% DMSO
Diluted in Fetal Bovine Serum

Table 2: Recipe for freezing medium

8.1.4   Observation and documentation

The cell growth and cell density was controlled every day with a light microscope. For documentation of drug effects pictures were with a Nikon Coolpix P5000 camera (Tokyo, JP).

8.2   Cell proliferation and cytotoxicity – MTT assay

Viability of cells was analysed by the EZ4U nonradioactive cell proliferation and cytotoxicity kit (Biomedica; Wien, AT). The assay is based on functional mitochondria of viable cells which convert MTT (3-(4,5-Dimethylthiazol-2-yl)—2,5-diphenyltetrazoliumbromide) to coloured formazan derivatives. The increase in absorbance allows quantification of viable cells. The assay was performed following the manufacturer's manual.

The day before drug treatment, SH-SHSY, Kelly and IMR-32 cells were seeded with a cell number of $2*10^4$ cells per well on a 96 well plate in 200 µl of the according growth medium. For each drug treatment, three wells with cells were prepared thus being able to measure the results in triplicates. As control, three wells per cell line were untreated and three wells with growth medium but lacking cells were used as a blank. The next morning, the medium was removed from the cells and fresh medium containing the drug in the desired dilution was added. After 72 hours of incubation, 20 µl of dye solution containing the MTT was diluted in 2.5 ml of activator solution and pipetted to each well. After further incubation of 2-5 hours at 37°C the optical density was measured by a plate reader set to 490 nm and 655 nm. The 655 nm value was used as a reference wavelength for correction of the background signal. Furthermore, the blank value was subtracted from the sample values and the results were normalized to the control with the control being the cells not treated with any drug as stated above.

8.3   Polymerase Chain Reaction – Analysis on RNA level

The three cell lines were treated with simvastatin and TNFα and after cell lysis total RNA was isolated, reverse transcribed to cDNA and analysed by PCR.

8.3.1   Preparation of cells

Cells were grown on 60 or 100 mm dishes for 24 hours before stimulation. After stimulation cells were incubated for 24 or 48 hours. Then, growth medium was collected in a labelled

falcon and cells were additionally washed with PBS and detached with trypsin-EDTA. After incubation for 5 minutes at 37°C cells were gathered using the collected growth medium and centrifuged at 900 rpm for 4 minutes at room temperature. The cell pellet was transferred into a tube and washed twice with cold PBS. The tubes were centrifuged at 1200 rpm for 4 minutes at 4°C.

8.3.2 Purification of total RNA

Total RNA was isolated from the cells using the RNeasy® Mini Kit by Qiagen (Basel, CH) following the manufacturer's protocol. To homogenize the cells they were vortexed vigorously and incubated for 5 minutes in an ultrasound bath. This process was repeated twice before continuing with the protocol. After elution of the purified RNA from the spin columns RNA yields and purity were determined with the Implen NanoPhotometer™ (Implen GmbH, München, DE).

8.3.3 DNase digestion and cDNA synthesis

DNase digestion was carried out with a Deoxyribonuclease I (Fermentas, Thermo Fisher Scientific Inc.; Massachusetts, USA Massachusetts, USA) according to the information provided. The resulting solution was directly used as a template for cDNA synthesis.
The RevertAid H Minus First Strand cDNA Synthesis Kit by Thermo Scientific (Massachusetts, USA) was applied for cDNA synthesis and manufacturer's protocol was followed. GAPDH control RNA provided with the kit was also reverse transcribed. cDNA concentrations and quality were determined using the Implen NanoPhotometer™ (Implen GmbH, München, DE).

8.3.4 PCR with specific primers

PCR was carried out with peqGOLD Taq-DNA-Polymerase "all inclusive" kit (PEQLAB Biotechnologie GmbH; Erlangen, DE). 150 ng of cDNA were mixed with the components provided with the kit (Table 3). The GAPDH cDNA was used for a positive control. The components only without any additional RNA template served as negative control. Samples were mixed with specific primers for the mRNA sequence of interest (Table 4) and with

primers for the housekeeping gene GAPDH. Finally, the PCR programme was run with 3 minutes of initial denaturation at 94°C and 35 cycles of denaturation at 94°C for 30 seconds, annealing at the temperature listed in Table 4 for 30 seconds and an extension period of 45 seconds at 72 °C.

cDNA	150ng
10x Reactionbuffer S	5 µl
5x Enhancer	10 µl
dNTPs (10mM)	1 µl
Fwd Primer (10µM)	1,5µl
Rev Primer (10µM)	1,5µl
Taq Polymerase (5U/µl)	0,25 µl
Water	Ad 50 µl

Table 3: Compounds for the PCR reaction with concentrations and volumes

mRNA	Primer forward 5'-3' sequence	Primer reverse 5'-3' sequence	Amplicon (bp)	Annealing Temperature (°C)
MYCN	CGCAAAAGCCACCTCTCATTA	TCCAGCAGATGCCACATAAGG	117	58
GAPDH	CAAGGTCATCCATGACAACTTTG	GTCCACCACCCTGTTGCTGTAG	490	54-59

Table 4: Specific Primers are listed here with forward and reverse sequence, amplicon size in bp and ideal annealing temperature in °C

8.3.5 Agarose gel electrophoresis and evaluation

Agarose gels were cast in the concentrations from 1-1.5% agarose in 1 x TAE buffer (Table 5) dyed with Serva DNA stain Green Clear G (Heidelberg, DE). The amplified samples were mixed with 6x DNA loading dye (Thermo Fisher Scientific Inc.; Massachusetts, USA) before applying them onto the gel. A 100 bp and a 1.000 bp Ladder by New England Biolabs (Massachusetts, USA) served as markers. The gels were run for 1 to 2 hours in 1 x TAE buffer at 80-100V. The gels were documented with the Bio-Rad Gel Doc 1000 System (Bio-Rad Laboratories Inc.; California, USA) and pictures stored as TIFF files.

Tris acetate EDTA buffer – TAE	
40mM	Tris
1mM	EDTA
Diluted in MQ, pH adjusted to 8,4 Autoclaved and stored at room temperature	

Table 5: Recipe for Tris-acetate-EDTA buffer

8.4 Transfection methods

8.4.1 Restriction digest of plasmids

Plasmids were checked before transformation and transfections by restriction digest. The eGFP, renilla and NFκB-luciferase plasmids (1 µg) were mixed with 1 µl of two single cutter restriction enzymes and 2 µl of the suitable buffer (Table 6). Volume was then brought to 20 µl with water and the mixture was incubated for 1.5 hours at 37°C and constant shaking. The DNA was stained with Serva DNA stain Green Clear G (Heidelberg, DE) and then separated in a 1% agarose gel. Samples were mixed with 6x DNA loading dye (Thermo Fisher Scientific Inc.; Massachusetts, USA) before applying them onto the gel. GeneRuler™ 1 kb

DNA Ladder (Thermo Fisher Scientific Inc.; Massachusetts, USA) served as marker and gel was run in 1x TAE buffer for 40 minutes at 130V.

DNA (1µg)	Buffer (2µl)	Enzyme 1 (1 µl=10U)	Enzyme 2 (1µl=10U)	Water
eGFP	Tango	NcoI	-	
Renilla	Tango	XbaI	NheI	Ad 20 µl
NFκB-luciferase	SdaI	NdeI	ScaI	

Table 6: Compounds for restriction digests of eGFP, renilla and NFκB-luciferase plasmids

8.4.2   Transformation of E. coli and plasmid DNA purification

Competent XL 10_*E. coli* cells (50-100 µl, stored at -80°C) and plasmid-DNA (stored at -20°C) were thawed on ice. 5 µg of plasmid DNA was merged with 50 µl of competent cells and the mixture was incubated on ice for 30 minutes. Subsequently, bacteria were heat-shocked for 60 seconds at 42°C. Cells were again left on ice for 5 minutes, after which they were suspended in 1 ml of LB medium (Table 7) and incubated for 1 h at 37°C and 450 rpm. Then, the tube with the cells was centrifuged for 3 minutes at 4000 rpm. The supernatant was discarded and the cells were plated on an LB-agar plate (Table 7) containing the antibiotic for selection of positive clones. The plate was incubated over night at 37°C. On the next day, a single colony was picked and transferred into 3 ml of LB medium containing the antibiotic for selection. This pre-culture was incubated for further 8 hours at 37°C while shaking. Afterwards, the cell-suspension was added to 250 ml of LB medium containing the selective antibiotic and again incubated over night at 37°C while shaking.

The plasmid DNA was purified using the HiSpeed® Plasmid Maxi Kit (Qiagen AG; Basel, CH) following the manufacturer's protocol.

LB Medium - Luria Bertani Medium	LB Agar– Luria Bertani Agar
1% Bactotryptone 0,5% Yeast Extract 1% NaCl	1,5% Agar
Diluted in MQ, pH adjusted to 7,0 Autoclaved and stored at 4°C	Diluted in LB medium Autoclaved and stored at 4°C

Table 7: Recipes for Luria Bertani (LB) medium and agar plates

8.4.3 Transfection with reagents

SH-SY5Y, Kelly and IMR-32 cells were plated on the required dishes, e.g. 6-well plates, the day before transfection. Number of cells for seeding was chosen so that the cells could reach 80% confluence until the next day, as the uptake of DNA is more efficient with cells being in the log growth phase. For example, for SH-SY5Y cells, a number of $5*10^5$ cells per well in a 6-well plate was chosen, while $1*10^6$ cells were seeded for IMR-32 and Kelly cells.

The transfection reagent and plasmid DNA was added to the cells according to the instructions provided with each reagent. Five hours after incubation with reagent and DNA cells were provided with fresh growth medium. All in all, cells were incubated for 48 hours after transfection. The following figure gives an overview of the general transfection workflow and the incubation periods (Figure 9).
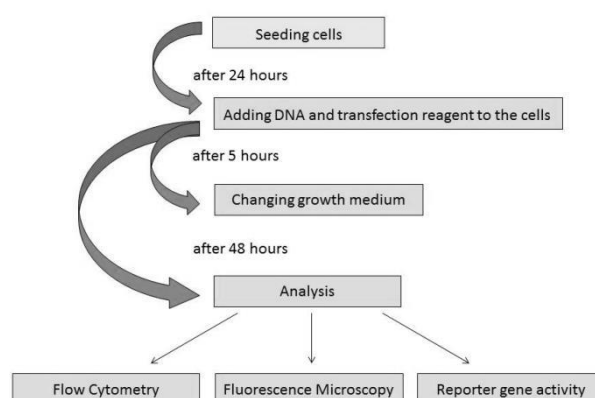

Figure 9: General transfection workflow

As most of the experiments were performed on 6-well plates, the following descriptions, concentrations and volumes all refer to this size of culture dish.

TurboFect™ (Thermo Fisher Scientific; Massachusetts, USA)

Transfection with the TurboFect™ reagent (Thermo Fisher Scientific Inc.; Massachusetts, USA) was performed according to the manufacturer's protocol. Per well, 200 µl of serum free growth medium were mixed with 0.6 µg of DNA before adding 0.6 µl of TurboFect™. The mixture was incubated for 15 minutes at room temperature and then added dropwise to the well. Cells were incubated for 5 hours at cell culture conditions before changing the growth medium. Transfection efficiency was explored after 48 hours.

X-tremeGene HP (Roche; Mannheim, DE)

Cells were transfected following the manufacturer's manual. 0.6 µg of DNA per well were mixed with 100 µl of serum free growth medium. 3 µl of X-tremeGene HP reagent (Roche; Mannheim, DE) were added, the mixture was incubated for 15 minutes at room temperature and then dropwise added to the well. Cells were incubated for 5 hours at cell culture conditions. Afterwards cells were provided with fresh medium. Transfection efficiency was measured after 48 hours of incubation.

X-tremeGene 9 (Roche; Mannheim, DE)

The transfection with X-tremeGene 9 (Roche; Mannheim, DE) was performed following the manufacturer's manual (see description above for X-tremeGene HP).

Viafect™ (Promega GmbH; Mannheim, Germany)

The transfection was conducted according to the manufacturer's manual. Per well, 3 µg of DNA were diluted in serum free medium and 9 µl of the Viafect™ reagent (Promega GmbH; Mannheim, DE) in order to reach a total volume of 300 µl. The mixture was incubated for 15 minutes at room temperature before adding it to the cells. The cells were incubated at cell culture conditions for 5 hours, the medium was changed and the cells were allowed to recover for 48 hours.

Fugene®6 (Promega GmbH; Mannheim, Germany)

The transfection was executed as recommended in the manufacturer's protocol. 9 µl of Fugene®6 reagent (Promega GmbH; Mannheim, DE) and serum free medium were incubated for 5 minutes before adding 3 µg of DNA in order to reach a total volume of 300 µl. After incubation of 15 minutes the mixture was added to the well. Cells were incubated for further 5 hours, the medium was changed and the cells were allowed to recover for 48 hours.

K2® Transfection System (Biontex Laboratories GmbH; München, DE)

Transfection was performed following the manufacturer's manual. 20 µl of the K2® Multiplier (Biontex Laboratories GmbH; München, DE) were mixed with 2 ml of fresh medium. The medium was removed two hours before transfection and the mixture was added to the cells. Per well, 4 µg of DNA and serum free medium were mixed to reach a volume of 50 µl. Furthermore, 16 µl of K2® reagent were added to 34 µl of serum free medium. Then, the both solutions were mixed and incubated for 15 min. In the end, the whole 100 µl were added dropwise to the cells. Cells were incubated for 5 hours at cell culture conditions before changing the medium. All in all, cells were incubated for 48 hours after transfection.

Calcium phosphate

This was the only transfection method tested which was performed without any acquired reagents. Thus, this protocol also deviates from the others. Cells must be fed in the morning. Transfection could then be started in the evening. For each well 10 µl of 2.5 M CaCl$_2$ were mixed with 100 µl of sterile H$_2$O before adding 0.6 µg of DNA. In another tube 100 µl of 2x HEBS (Table 8) was prepared and air was blown into the solution using a pipette. Subsequently, the DNA mix was dropwise added to the 2 x HEBS and immediately afterwards added to the culture medium on the plate. Cells were incubated overnight at cell culture conditions. The next morning growth medium was removed from the treated cells and 200 µl of 15% Glycerol in PBS was added to each well. Afterwards the Glycerol was further diluted by adding 2 ml of PBS to the well. The Glycerol-PBS mixture was removed and growth medium was added. Cells were allowed to recover for 48 hours.

2 x HEBS - HEPES buffered saline	
2,8 ml	2M NaCl
2 ml	0,5M HEPES, pH 7
60 µl	0,5M $Na_2HPO_4*2\ H_2O$
15,2 ml	H_2O
pH adjusted to 7,1	
Sterile filtered and stored at -20°C	

Table 8: Recipe for 2 x HEBS, HEPES buffered saline

8.4.4   An instrumental transfection method: Electroporation

Electroporation with Bio-Rad-GenePulser Xcell™ - Exponential decay protocol
First, $2*10^6$ cells were re-suspended in 400 µl of cold Dulbecco's Modified Eagle's Medium with 10% FBS (w/o phenol red, Sigma Aldrich; Missouri, USA) and mixed with 20 µg of DNA. The sample was transferred into a 4 mm electroporation cuvette (Bio-Rad Laboratories Inc.; California, USA) and electroporated with 200 V, 1200 µF and a resulting pulse length of 35-40 msec. Cells were then mixed with 4 ml of medium and split into 2 wells of a 6-well plate. The growth medium was changed after 5 hours and cells were incubated for 48 hours.

Electroporation with Bio-Rad-GenePulser Xcell™ - Square wave protocol
For this protocol, $1.5*10^6$ cells were re-suspended in 400 µl of Dulbecco's Modified Eagle's Medium with 10% FBS (w/o phenol red, Sigma Aldrich; Missouri, USA) and mixed with 10 µg of DNA. Cells were electroporated in a 4 mm electroporation cuvette (Bio-Rad Laboratories Inc.; California, USA) at 200 V for 20 msec with a square wave pulse.

8.5   Fluorescence activated cell sorting analysis - FACS

8.5.1   Fixation of cells

For fixation of cells the growth medium was collected in a tube and cells were washed with PBS. Thereafter, cells were treated with trypsin-EDTA and incubated for about five minutes at 37°C. The cell suspension was then collected by adding the previously removed medium to each well and pipetting it back into the tube. Cells were pelleted by centrifuging at 900 rpm for 4 minutes. Falcons were put on ice and cells were washed with PBS. The cell pellet was re-suspended in 250 µl of cold 4% Formaldehyde in 0.8% NaCl and incubated on ice for 10 minutes. Subsequently, 250 µl of PBS were added to the suspension.

8.5.2   Flow Cytometry and evaluation

To analyse the efficiency of transfection by Flow cytometry, cells were transfected with eGFP plasmid. The amount of protein, Green Fluorescent Protein (GFP), could be measured using a FACS Canto II (V96100032; New Jersey, USA) set at excitation wavelength 488 nm and an emission at 515 nm. With FACS DIVA software (BD biosciences; San Jose, USA) data were transformed into a histogram which allowed determining the geometric mean of the intensity of GFP. In addition the Cyflogic.exe software could then be used for further analysis. The results for transfection were expressed as fold of control, the control being the cells which had not been transfected.

8.6   Fluorescence Microscopy

8.6.1   Preparing cells for Fluorescence Microscopy

Before adding cells to the according dish sterile cover glasses were put into it so that cells could attach while growing. After the transfection with eGFP plasmid DNA and the recovery of cells, nucleic acid Hoechst stain was added (1:2.000) to the growth medium and incubated for 10 minutes at 37°C. Cells were washed with PBS for three times and then incubated with

4% formaldehyde in 0.9% NaCl for 10 minutes. Thereafter, formaldehyde was removed and cells were again washed three times with PBS. Mowiol mountain medium was used to attach the cover glasses upside down onto object slides. The edges were sealed with nail polish. Cells on object slides were stored at 4°C.

8.6.2 Microscopy

Pictures were taken with LSM 510 Confocal Microscope (Molecular Imaging Unit; Helsinki, FI) and LSM 510 Meta 3.2 Software (Molecular Imaging Unit; Helsinki, FI). Transfection efficiencies were evaluated using ImageJ software. As the results for transfection efficiencies were very low due to high background signal and therefore not comparable to FACS results these data were excluded from the evaluation process (Figure 10).
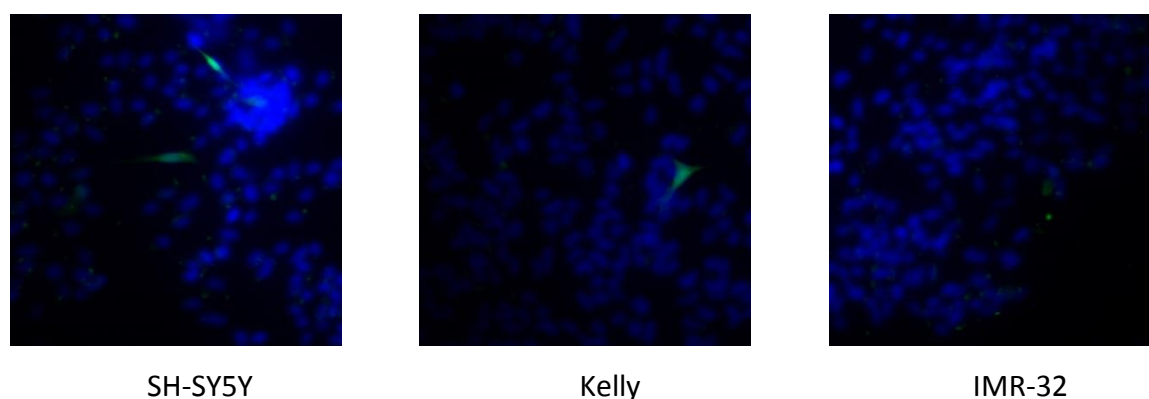
| SH-SY5Y | Kelly | IMR-32 |

Figure 10: Transfected SH-SY5Y, Kelly and IMR-32 cells.
Blue colour indicates the Hoechst stained nuclei and green fluorescent cells are successfully transfected cells expressing eGFP protein.

8.7 Luciferase reporter assay

Luciferase reporter assays were not only performed to have a further result for transfection efficiencies but mainly to study effects of drug treatments on gene regulation. Cells were

transfected with plasmid DNA containing the luciferase gene with a promoter region of a gene of interest and additionally with plasmid DNA containing the renilla gene for normalization of transfection. One day after the transfection, cells were treated with drugs in different concentrations and incubated for 48 hours. The assay was evaluated using the Firefly & Luciferase Assay Kit by Biotium (California, USA) following the manufacturer's manual. The 5x Lysis buffer provided with the kit was diluted in MQ. Each culture well was washed with PBS before adding Lysis Buffer. The plates were incubated at room temperature for 15 minutes while shaking. Renilla and luciferase signals had to be measured separately. Therefore, two luminometer plates were prepared: On the plate for renilla signal, 25 µl of renilla enhancer was added to each well. Then 20 µl of lysate was pipetted to the wells and just before measurement 25 µl of renilla substrate, coelenterazine, was added. For the firefly measurement 20 µl of lysate with 50 µl of luciferase substrate, D-luciferin, were prepared on the plate. Luminescence was measured and results were normalized with the renilla signal. The results were expressed as fold of control.

8.8 Protein analysis

8.8.1 Cell treatment

For observation of effects due to different drug treatments on protein expression cells were grown on 60 mm dishes with a cell number that allowed them to reach 80 % confluence until cell lysis. After 24 hours growth medium was removed and fresh medium containing drugs or combination of drugs in different concentrations was added. Cells were incubated for further 48 hours until cell lysis.

8.8.2 Cell lysis

The dishes were put on ice. The medium was transferred into a falcon and centrifuged at 1.4 krpm for 4 minutes at room temperature. Subsequently, the dish was washed twice with PBS. Hereafter, liquid nitrogen was poured onto the dish to shock-freeze the cells. For cell lysis 80 µl of IP lysis buffer (Table 9) were pipetted onto the plate, spread with a scratching

tool and incubated for 10 minutes on ice. The cell pellet in the falcon was washed with PBS and centrifuged at 7 krpm for 8 minutes at 4°C. The IP buffer with cells from the dishes was used to re-suspend the according cell pellet. The tubes containing the mixture were frozen in liquid nitrogen and rewarmed in the water bath set at 37°C. This step was repeated twice, followed by 10 seconds of ultrasonic bath. In the end, proteins and cell debris were separated by centrifuging the tubes at 15 krpm for 40 minutes at 4°C. The supernatant containing protein was transferred into a labelled tube which was stored at -20°C.

IP lysis buffer	
25 mM	Tris-HCl (pH 7,5)
150 mM	NaCl
10 mM	EDTA
0,1%	Triton X-100
0,5%	NP-40
10 mM	Glycerolphosphate
Stored at -20°C	

Table 9: Recipe for IP Buffer

8.8.3 Protein concentration measurement

Protein concentrations were determined by using the Bio-Rad Protein Assay Dye Reagent Concentrate (Bio-Rad Laboratories Inc.; California, USA). The solution was prepared as a 1:5 dilution as recommended in the manufacturer's manual. For the measurement 7 µl of each sample were added to 1000 µl of diluted Bio-Rad solution. Samples were always measured in duplicates. 7 µl of water and 7 µl of IP buffer served as blank values. The optical density of the mixture could then be determined with a photometer set at 595 nm. Concentrations were used to determine equal amounts of protein to apply on the SDS gels.

8.8.4 Sodium Dodecyl Sulphate Polyacrylamide Gel Electrophoresis - SDS-PAGE

The SDS gels were cast using the Bio-Rad Mini-PROTEAN® Tetra Cell equipment (California, USA). 10 or 15 well combs and 0.75 mm or 1 mm spacers were applied depending on the volume and number of protein samples. The percentage of acrylamide-bisacrylamide of the gel allows controlling the separation process and must thus be chosen according to the size of the protein of interest (Table 10).

Protein MW (kDa)	Gel percentage (%)
4-40	20
12-45	15
10-70	12.5
15-100	10
25-200	8

Table 10: Acrylamide-bisacrylamide percentage of the gel has to be chosen according to the size of the protein of interest to reach an ideal separation

The compounds and recipes for the SDS-PAGE gels are listed in Table 11 and Table 12. The separating gel was cast first and isopropanol was used to even the surface. After the gel had polymerized isopropanol was removed and stacking gel was cast on top of the separating gel, inserting the comb with the number of wells required. The gel was allowed to polymerize at room temperature. After polymerization the gel could either be directly used or stored at 4°C wrapped in soaked paper towels and covered with foil.

1,5 M Tris-HCl Buffer	0,5 M Tris-HCl Buffer
1,5 M Tris-HCL	0,5M Tris-HCl
Diluted in MQ, pH adjusted to 8,8 Stored at 4°C	Diluted in MQ, pH adjusted to 6,8 Stored at 4°C

10% SDS	10% Ammonium Persulfate
10% (m/v) Sodium Dodecyl Sulfate	10% (m/v) Ammonium Persulfate
Diluted in MQ Stored at 4°C	Diluted in MQ Stored at 4°C

Table 11: Compounds of SDS-PAGE gels

Separating Gel (volumes in µl)	7%	8%	9%	10%	11%	12%	13%	15%
1.5M Tris (pH 8.8)	2500	2500	2500	2500	2500	2500	2500	2500
10% SDS	100	100	100	100	100	100	100	100
H_2O	4960	4620	4290	3960	3630	3290	2960	2290
30%-0,8% Acryl-Bisacryl	2330	2670	3000	3330	3660	4000	4330	5000
10% Ammonium Persulfate	100	100	100	100	100	100	100	100
TEMED	10	10	10	10	10	10	10	10
Total Volume - 10 ml								

Stacking Gel (Volumes in µl)	3%	5%
0,5 M Tris (pH 6.8)	1250	1250
10% SDS	50	50
H_2O	3150	2810
30%-0,8% Acryl-Bisacryl	500	835
10% Ammonium Persulfate	50	50
TEMED	5	5
Total Volume – 5 ml		

Table 12: Recipes for casting separating and stacking gels for SDS-PAGE

Gels were moved into the tank of the Bio-Rad Mini-PROTEAN® Tetra Cell Electrophoresis Module (California, USA). It was filled with cold 1 x Running Buffer (Table 13). Before loading the samples were diluted in 4 x Sample Buffer (Table 14) and heated to 95°C for 5 minutes at 450 rpm. In addition to the samples the Spectra™ Multicolor Broad Range protein ladder (Thermo Fisher Scientific; Massachusetts, USA) was applied onto the gel. Gels were run with a constant voltage of 150 V for approximately 2-3 hours.

10 x Running Buffer	
250 mM	Tris-HCl
1,92 M	Glycin
10 mM	EDTA.Na$_2$
1%	SDS

Diluted in MQ, pH adjusted to 8,3
Stored at room temperature

1 x Running Buffer	
10% (v/v)	10 x Running Buffer

Diluted in MQ
Stored at 4°C

Table 13: Recipes for 10 x and 1 x Running Buffer

4 x Sample Buffer	
60mM	Tris-HCl (pH 6,8)
14,4mM	Mercaptoethanol
25%	Glycerin
2%	SDS
0,1%	Bromphenolblue

Diluted in MQ
Stored at -20°C

Table 14: Recipe for 4 x Sample Buffer

8.8.5 Western Blotting

Wet blotting was performed using the Bio-Rad Mini Trans-Blot®Electrophoretic Transfer Cell (California, USA). Fibre pad, filter paper, the gel and a nitrocellulose membrane, another layer of filter paper and fibre pad were all soaked in 1 x Transfer buffer (Table 15) and put together layer by layer avoiding the formation of air bubbles. The assembled layers were placed into the gel holder cassette. A cooling unit, the gel holder cassette and the electrode module were placed into the tank. The tank was filled with cold 1 x Transfer Buffer and the device was set to constant 150V. The blot was run for 1 hour.

10 x Transfer Buffer	
250 mM	Tris-HCl
1,92 M	Glycin
1%	SDS

Diluted in MQ, pH adjusted to 8,3
Stored at room temperature

1 x Transfer Buffer	
10% (v/v)	10 x Transfer Buffer
20%	Methanol

Diluted in MQ
Stored at 4°C

Table 15: Recipes for 10 x and 1 x Transfer Buffer

The washing and incubation steps after Western blotting are summarized in Table 18. The nitrocellulose membrane was washed twice in H_2O to remove any possible residues and subsequently stained with Ponceau S solution for several minutes. Like this proteins transferred from the gel onto the membrane are stained. Therefore, this step presents a control of the blotting process. The stained blots were scanned and saved as JPEG files. The dye was washed off the membrane with TBS Buffer (Table 16). To avoid unspecific binding, the blot was blocked with 5% BSA in TBST solution (Table 17) for minimum 2 hours or overnight.

10 x TBS	
0,2 M	Tris-HCl
1,5 M	NaCl

Diluted in MQ, pH adjusted to 7,5
Stored at room temperature

1 x TBS	
10% (v/v)	10 x TBS

Diluted in MQ
Stored at room temperature

Table 16: Recipes for 10 x and 1 x TBS

1 x TBST	
10% (v/v)	10 x TBS
0,2% (v/v)	Tween
Diluted in MQ	
Stored at room temperature	

Table 17: Recipe for 1 x TBST

Specific antibody binding was applied as method of detection. The primary antibody was diluted 1:500-1:2.000 in 2% BSA in TBST with 0.1% NaN_3. Then, the blot was incubated overnight at 4°C with the antibody specific for the protein of interest. On the next day, the membrane was washed three times with TBST Buffer for 15 minutes at room temperature. The secondary antibody was diluted 1:5.000-1:10.000 in 2% BSA in TBST added to the membrane and incubated at room temperature for one hour. The secondary antibody, linked to a horse reddish peroxidase, binds species specifically to the primary antibody. Hereafter, the blot was again washed three times with TBST Buffer for 15 minutes. In the end, the membrane was washed with TBS Buffer for 20 minutes.

2x	3 min	H$_2$O wash
		Ponceau Staining
2x	3 min	TBS wash
	2 h	Blocking in 5% BSA in TBST
	Overnight (at 4°C)	1st Antibody (1:500-1: 1.000) in 2% BSA in TBST with 0.1%NaN$_3$
3x	15 min	TBST
	1 h	2nd Antibody (1:5.000-1:10.000) 2% BSA in TBST
3x	15 min	TBST
1x	20 min	TBS

Table 18: Overview of the washing and incubation steps after Western blotting.
If not indicated otherwise, steps were performed at room temperature.

As mentioned before, the secondary antibodies are linked to an enzyme, namely horse reddish peroxidase. The great advantage of this detection method is that the employment of hazardous radioisotopes can be avoided. Providing the enzyme with a substrate it produces a luminescent signal witch can darken a photographic film and thus makes visible the protein bound by the linked antibody. Two different substrate solutions were applied: the Thermo Scientific SuperSignal® West Pico Chemiluminescent Substrate (Thermo Fisher Scientific Inc.; Massachusetts, USA) usually delivers a signal less intense than the Amersham™ECL™ Prime Western Blotting Detection Reagent (GE Healthcare; Buckinghamshire, UK). The substrate must be chosen depending on the amount of protein present in the sample. The two substrates were prepared identically: A provided luminol and peroxide solution had to be mixed 1:1 just before application. The reaction "enhanced chemiluminiscence (ECL)" takes place, meaning the peroxidase oxidises the luminol and delivers a light emission. A CL-XPosure film (PI-34089; THP Medical Products Vertriebs GmbH; Wien, AT) was placed onto the membrane. With different exposure periods the intensity of the signal could be varied. In the end, the film was developed.

For quantification of Western Blots the developed films were scanned and saved as JPEG and TIFF files. With the freeware ImageJ software the files were first converted to 8-bit type and then analysed with the function "Gels - Select Lane - Plot lanes" which allows comparing the areas of horizontal bands on a plot. At least two films with different exposure times were

evaluated. The normalization to the loading control (if possible) and the calculation of means and standard deviations was performed in Microsoft Excel.

8.9 Statistical analysis

Data were statistically analysed with "One way ANOVA analysis" for multiple comparison and post-hoc Dunett's test in *GraphPad Prism.* Statistical significances are indicated as n.s. : not significant or $p > 0.05$, * : $p < 0.05$, ** : $p < 0.01$, *** : $p < 0.001$.

9   Results

9.1   Simvastatin effects on three neuroblastoma cell lines

Statins, HMG-CoA reductase inhibitors, are drugs with pleiotropic actions (see section 7.3 "Statins and their pleiotropic effects"). Among others they have been investigated as chemopreventive drugs due to their anti-cancer effects. Different studies already proved this assumption.[48,68] Statins were shown to be effective in rhabdomyosarcoma cells in combination with doxorubicin and therefore proposed as supplementary drugs to chemotherapeutics in patients with ABCB1-mediated multidrug resistance.[69,70] Also in metastatic melanoma cells simvastatin was proven to be involved in apoptotic events.[71] Lovastatin was shown to induce apoptosis in SH-SY5Y cells, a NB cell line without MYCN amplification.[72]

This study aimed among others to identify simvastatin effects on MYCN amplified NB cell lines. Three different primary human NB cell lines were cultured for all the experiments. The SH-SY5Y cell line has no MYCN amplification and is sensitive to statin treatment which has been investigated in previous experiments. MYCN amplification is a genetic marker in NB associated with poor prognosis for the patients (see section 7.2 "Myc - Family of proto-oncogenes") and therefore the two MYCN amplified cell lines, Kelly and IMR-32, were used for comparison.

Already after treatment with 3 µM simvastatin for 48 hours the morphology of the cells revealed the different susceptibilities of the three cell lines (Figure 11). While SH-SY5Y cells get rounded and detach in the presence of 3 µM simvastatin, Kelly and IMR-32 cells did not really appear to be affected morphologically by this treatment.
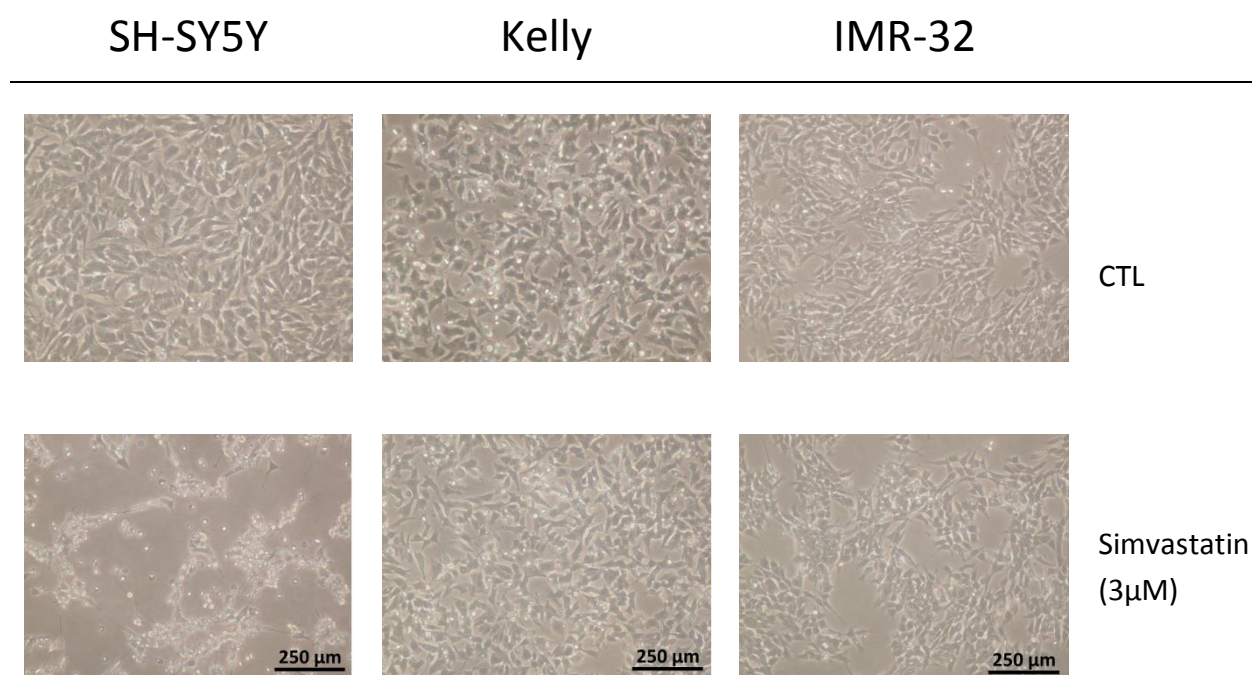
Figure 11: Different susceptibility to simvastatin of SH-SY5Y, Kelly and IMR-32 cells.
SH-SY5Y cells, Kelly and IMR-32 cells were exposed to 3 µM simvastatin (Sim) for 48 hours and compared to untreated controls (CTL). Pictures were taken on a Nikon microscope at a magnification of 10x.
Scale bar = 250 µm

9.2 Different MYCN and N-Myc concentrations on m-RNA and protein level are confirmed

In order to confirm the different N-MYC status in these three cell lines MYCN amplification was investigated on mRNA and protein level.

First, a PCR of total RNA isolates with MYCN specific primers was conducted to prove that MYCN is amplified in Kelly and IMR-32 cells. Same concentrations of cDNA transcripts were employed to compare the results (Figure 12). The 117 bp MYCN amplicon is detectable in all three cell lines but is only a faint band in SH-SY5Y cells. In comparison, the housekeeping gene GAPDH was equally detectable in all three cell lines. However, Kelly cells seem to have less MYCN mRNA than IMR-32 cells.
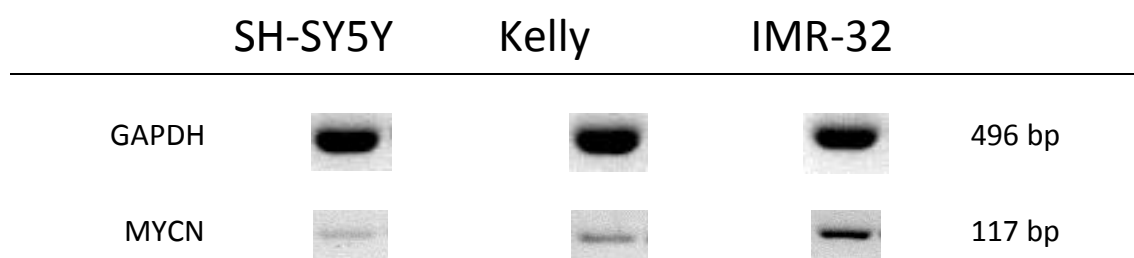
Figure 12: Comparison of MYCN mRNA in SH-SY5Y, Kelly and IMR-32 cells.
Equal amount of cDNA from SH-SY5Y, Kelly and IMR-32 cells were run for PCR to detect the MYCN amplicon 117 bp which was compared with the GAPDH amplicon (496 bp) on a 1.5% agarose gel.

Moreover, to clarify that MYCN amplification is also converted into higher amounts of N-Myc protein in Kelly and IMR-32 cell lines Western blot analysis was conducted (Figure 13). Therefore, total protein cell lysis was performed and proteins were separated with SDS-PAGE. N-Myc protein was detected with polyclonal N-Myc specific rabbit antibodies and a second species specific antibody linked to a horse reddish peroxidase enzyme provided with an ECL substrate. The same exposure times revealed the different concentrations of protein present in the cells.

	SH-SY5Y	Kelly	IMR-32	
N-Myc				60-64 kDa
				50 kDa
α-Tubulin				50 kDa
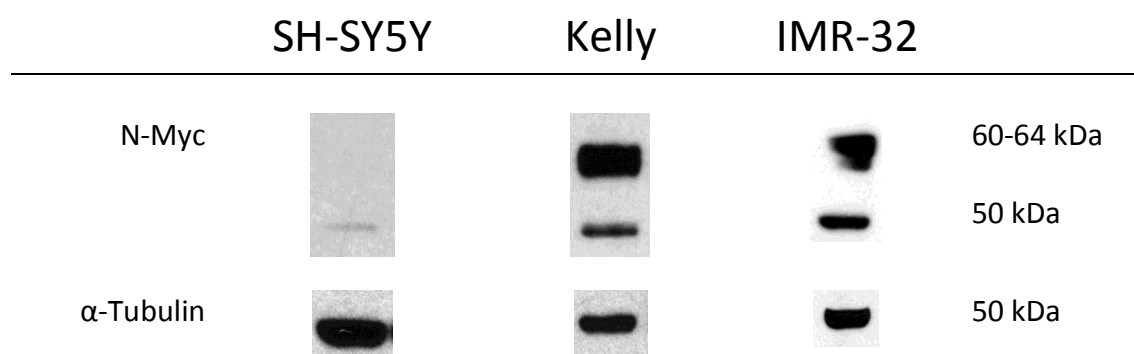
Figure 13: Western blot analysis for N-Myc protein in total protein lysates of SH-SY5Y, Kelly and IMR-32 cells. Equal amounts of cell lysates (15 µg) from SH-SY5Y, Kelly and IMR-32 cells were resolved on a 13% SDS-PAGE, transferred to nitrocellulose and probed for N-Myc and α-Tubulin as loading control. The molecular mass of the proteins is indicated and a representative experiment is depicted.

On the exposed X ray film N-Myc appears as double band in the 64 kDa region. This might be explained by cross-reactivity with the highly conserved c-Myc homologue. Nevertheless, this assumption might not be correct, since c-Myc should be detectable in SH-SY5Y cells, which is clearly not the case. Alternatively, Mäkalä *et al.* proposed that N-Myc and the phosphorylated N-Myc migrate in the range from 58 kDa to 64 kDa. In addition two AUG translation initiation sites separated by 24 bp in the second exon may further explain different protein species.[73]

In all three cell lines a 50 kDa band is recognized in N-Myc Western blots. This protein is considered to be unspecific. Nevertheless, it is also detectable in SH-SY5Y cells.

9.3 Transfection experiments with GFP

9.3.1 *Restriction digest – Positive identification of the employed plasmids*

NB cell lines are known to be difficult to transfect. It was therefore the aim of this work to evaluate various non-viral transfection methods. The three different plasmids used in this transfection experiments were first characterized and digested with the according restriction enzymes to ensure their identity (Figure 14). The eGFP plasmid was further used for evaluation of transfection methods and thereafter the renilla and NFκB-luciferase plasmids were used in luciferase reporter gene assays.

DNA fragments were applied onto a 1% agarose gel run in 1x TAE buffer for separation which is shown in Figure 14. A 1 kb Ladder was used as marker. The 4045 bp renilla plasmid was digested with the single cutter endonucleotidases XbaI and NheI into fragments with the anticipated lengths of 3098 bp and 947 bp. The digest of the 5695 bp 5x NFκB-Luciferase plasmid with NdeI and ScaI enzymes resulted also in the expected fragment lengths of 4200 bp and a 1495 bp. And the restriction digest of the 4733 bp eGFP-N1 plasmid with NcoI enzyme led to fragments of 1904 bp, 1809 bp appearing as one band on the gel, and in addition to 703 bp and 317 bp fragments. The smallest of the fragments is hardly visible, which may be explained by the low concentration of the agarose gel. Nevertheless, the identity of the three tested plasmids could be confirmed.
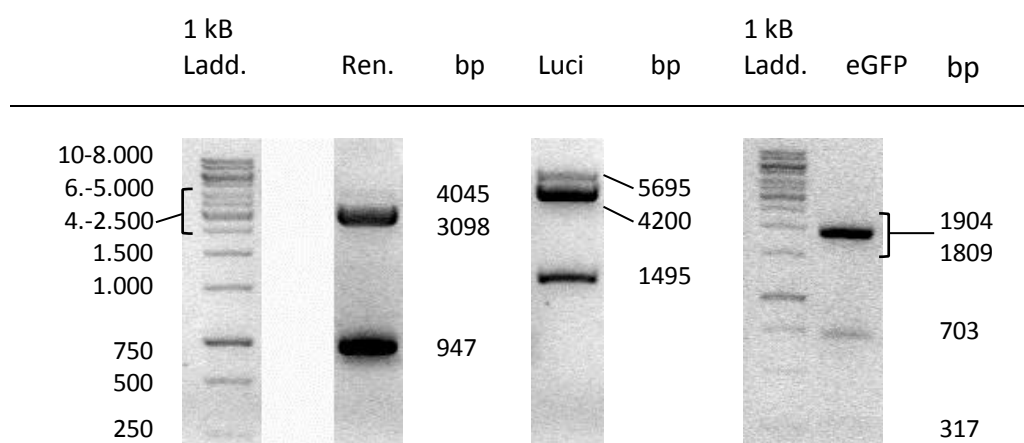
Figure 14: Restriction digests of renilla (Ren), 5x NFκB-luciferase (Luci) and eGFP-N1 (eGFP) plasmids.
Renilla plasmid was digested with XbaI and NheI, 5x NFκB-luciferase plasmid with NdeI and ScaI and eGFP-N1 plasmid with NcoI enzymes. After the digest the resulting DNA fragments were separated on a 1% agarose gel run in TAE buffer at 130V for 40 minutes. A 1kb ladder (Ladd.) was applied as marker.

9.3.2 Transfection efficiencies – Reagent based methods vs. electroporation

To evaluate the efficiencies of different transfection reagents and the instrumental electroporation method the three NB cell lines were transfected with an eGFP-N1 plasmid. The transfection efficiencies were determined measuring the GFP emission by flow cytometry 48 hours after transfection.

The reagent based methods did not lead to satisfying results as the 10% threshold could not be exceeded with calcium precipitation, TurboFect™, Xtreme HP, Xtreme 9, Viafect™ and Fugene®6. The findings are summarized in Figure 15. Only one reagent could convince, namely the K2® transfection system by Biontex. With K2® the transfection efficiencies reached the significant values of 20.91% ± 1.49% for SH-SY5Y cells, 12.87% ± 1.64 for Kelly cells and 14.29% ± 3.43% for IMR-32 cells.
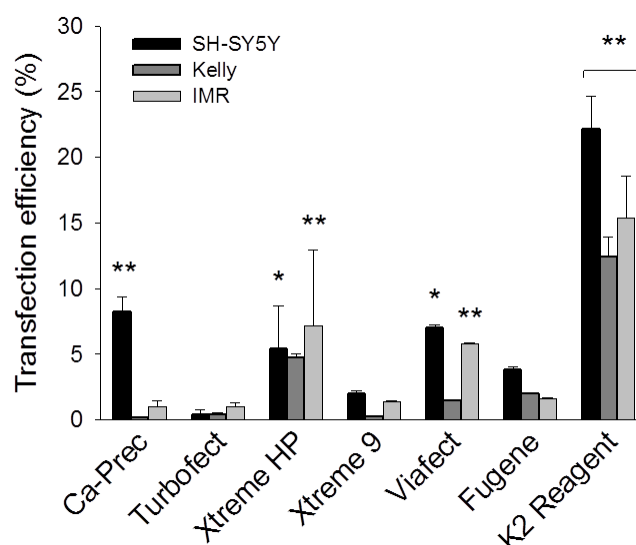
Figure 15: Transfection efficiencies using various reagent based methods in SH-SY5Y, Kelly and IMR-32 cells. Calcium precipitation (Ca-Prec, n = 4), TurboFect™ (n = 2), Xtreme HP (n = 3), Xtreme 9 (n = 2), Viafect™ (n = 2) and Fugene®6 (n = 2) reagents were used to evaluate the transfection efficiency. The 10% threshold was clearly reached with the K2® transfection reagent kit (n = 4). Results were analysed with FACS DIVA software and Cyflogic.exe software. Transfection efficiencies were compared to untransfected cells and expressed in %. Error bars denote SD (* : p<0.05, ** : p<0.05).

The K2® transfection kit was then compared to electroporation (Figure 16). For this mechanical method square wave pulse as well as exponential decay protocols were applied which both led to similar results. In SH-SY5Y cells electroporation showed the best transfection efficiency with 58.1% ± 11.19%. Besides, 13.25% ± 8.62% of Kelly cells could be transfected and 10.26% ± 5.74% of IMR-32 cells. The problem with this method is obvious. Only the K2® reagent transfection method results in comparable l transfection levels in all three cell lines.
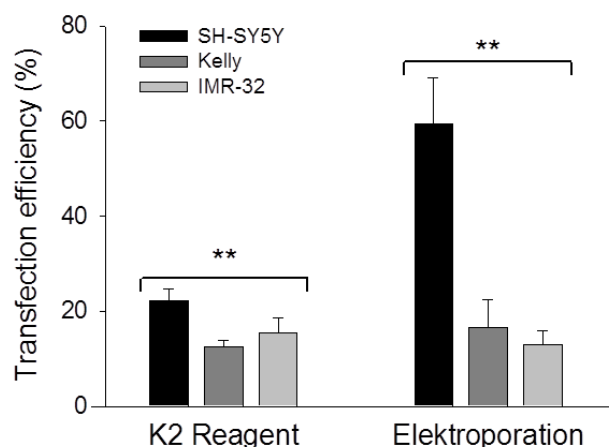
Figure 16: Transfection efficiencies with K2®reagent and electroporation in comparison for SH-SY5Y, Kelly and IMR-32 cell lines.
Transfection efficiencies were determined by flow cytometry 48 hours after transfection with the laser set at Alexa 488 nm. Results were analysed with FACS DIVA software and Cyflogic.exe software. Transfection efficiencies were compared to not transfected cells and expressed in %. Error bars denote SD; * : $p<0.05$, ** : $p<0.05$ (n = 4)

9.4 NFκB-luciferase Reporter Assay

9.4.1 Inflammatory events could be triggered in SH-SY5Y but not in Kelly and IMR-32 cells

The expression of the multifunctional transcription factor NFκB which presents a link between inflammation and cancer was studied on transcriptional level after treatment of cells with TNFα, simvastatin and trichostatin A (TSA). Cells were transfected with NFκB-luciferase plasmids as well as renilla plasmids. The Biotium Firefly & Renilla Dual Luciferase Kit was applied to supply the enzymes with the according substrates to consecutively measure the luminescence from renilla and luciferase. The blank value was subtracted from samples and divided by renilla luminescence, allowing normalization of the signalling with respect to the transfection efficiency. The summarized values are depicted in Figure 17 and expressed as fold of control.
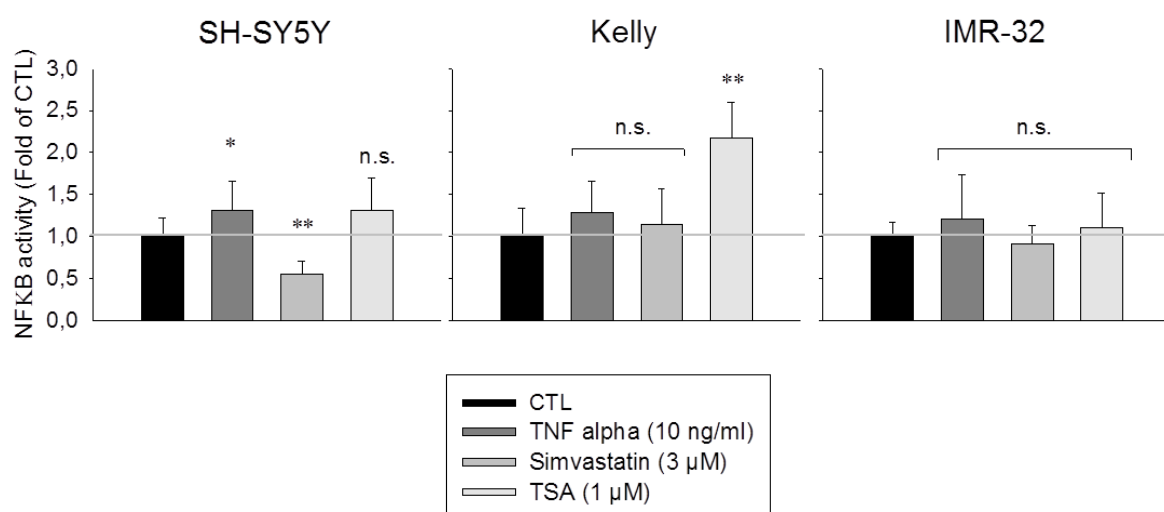
Figure 17: Summary of luciferase reporter assay results for NFκB activity in SH-SY5Y, Kelly and IMR-32 cells.
The three cell lines were treated with 10 ng/ml TNFα (SH-SY5Y n = 5, Kelly n = 5, IMR-32 n = 3), 3 μM simvastatin (SH-SY5Y n = 5, Kelly n = 4, IMR-32 n = 3) and 1 μM TSA (SH-SY5Y n = 3, Kelly n = 4, IMR-32 n = 4) for 48 hours before evaluation. The control sample (CTL) was not treated with any drug. After subtraction of the blank value, luciferase was divided by renilla signal for normalization. Results are shown as fold of control (CTL) values. Error bars denote SD; n.s : not significant, * : $p<0.05$, ** : $p<0.05$

In SH-SY5Y cells NFκB activity was significantly lowered to 0.56 ± 0.15 when treated with 3 μM simvastatin for 48 hours. The positive control for inflammation treated with 10ng/ml TNFα indicates a light but significant increase of NFκB activity to 1.31 ± 0.35. Such a regulation was not observed in N-Myc amplified cell lines. For Kelly and IMR-32 cell lines on the other hand no significant results could be detected except for the high increase of NFκB activity to 2.17 ± 0.42 with TSA treatment which at the moment is difficult to explain.

9.4.2   No apparent regulation of NFκB activity on protein level

Possible regulation of NFκB on protein level was evaluated with Western blot analysis of such treated cells. The NFκB p65 subunit was detected in 10 ng/ml TNFα and 3 μM simvastatin cells and compared with controls. No regulation on the protein level of NFκB is visible in Figure 18. Housekeeping gene α-Tubulin served as control.

	SH-SY5Y			Kelly			IMR-32		
TNF-α (ng/ml)	-	10	-	-	10	-	-	10	-
Sim (µM)	-	-	3	-	-	3	-	-	3

NFκB (p65)   50-52 kDa

α-Tubulin   50 kDa
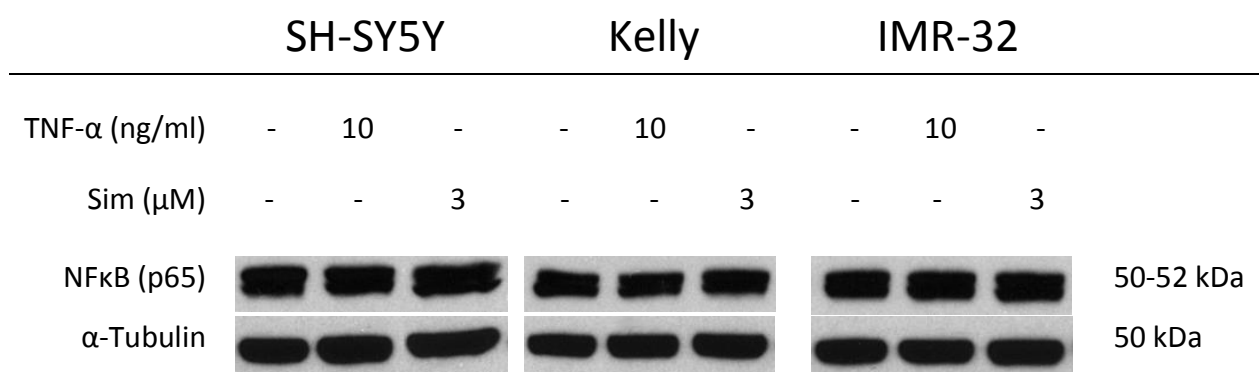
Figure 18: Western blot analysis of NFκB (p65) protein in SH-SY5Y, Kelly and IMR-32 cells.
Proteins were isolated from total cell lysates after 48 hours of treatment with Tumour necrosis factor α (TNFα) and simvastatin (Sim). α-Tubulin served as control and appears at 50 kDa, NFκB shows a double band at 50-52 kDa. Representative blots are shown from experiments which were repeated three times.

9.5 Viability and Cytotoxicity assay

Luciferase reporter assays for NFκB activity showed that inflammatory events could not be triggered by TNFα in N-Myc amplified cell lines. That is why further experiments aimed to screen for other possible drug targets. With the performance of MTT assays (EZ4U Nonradioactive cell proliferation and cytotoxicity assay; Biomedica, Wien, AT) different drugs and combinations should be tested for their ability to cause apoptosis in SH-SY5Y, Kelly and IMR-32 cell lines.

The drugs applied for these experiments were chosen because they had been proven to be effective in previous experiments like simvastatin. But also new promising drugs were tested such as the ALK inhibitor TAE-684 or the aurora kinase inhibitor VX680 (see section 7.1.3 "NB-Common treatment options and possible new approaches"). Furthermore all these drugs were applied in combinations with each other to identify possible synergy effects.

For all the following experiments samples were carried out in triplicates. Cells were grown for 24 hours on 96 well plates before treatment and then incubated for further 48 to 72 hours. For drug treatment the according amount of substances diluted in maximum 0.1% DMSO was mixed with the prepared medium and then added to the cells. Measurement was performed after another 4 hours of incubation with the substrate

provided in the kit. Wavelength for the measurement was 490 nm and 655 nm served as reference wavelength. The results from measurement at reference wavelength were subtracted from the results gained with the measurement at 490 nm. Data are expressed as fold of control.

9.5.1 DMSO does not have an effect on cell viability in concentrations below 0.5%

In order to control for the solvent and solvent effects DMSO was added to the cells in increasing concentrations. Figure 19 comprises the summarized results.
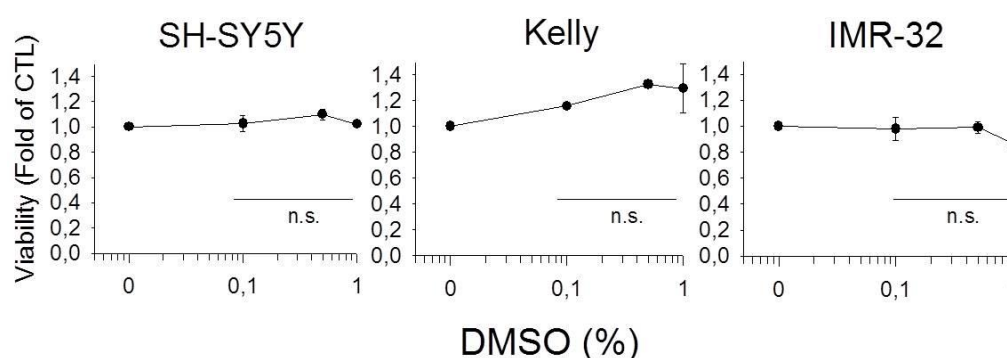
Figure 19: Viability of SH-SY5Y, Kelly and IMR-32 cells after 72 hours of DMSO treatment.
DMSO was applied in concentrations from 0% to 1%. The results did show that DMSO does not have a negative effect on the viability of the three cell lines. Results were analysed at 490 nm and at 655 nm served as reference measurement. Samples were all carried out as triplicates. The reference values were subtracted from the 490 nm values. Results represent the mean of fold of control values. Error bars denote SD; n.s. : not significant; n : 3

Evaluation of those viability assays clarified that DMSO definitely has no effects on the three cell lines below 0.5%. Consequently, DMSO was not used above 0.1%.

9.5.2 Simvastatin brings down SH-SY5Y but not Kelly and IMR-32 cells

Simvastatin has already been shown to affect the viability of SH-SY5Y when cells were in culture (Figure 11). These data could be also confirmed by viability assays (Figure 20). Simvastatin significantly reduced the viability of SH-SY5Y cells. A concentration of 1 µM

simvastatin reduced the population of living cells to about 40% and with 3 µM to even 15%. Viability of Kelly and IMR-32 cells on the other hand was not affected by this drug.
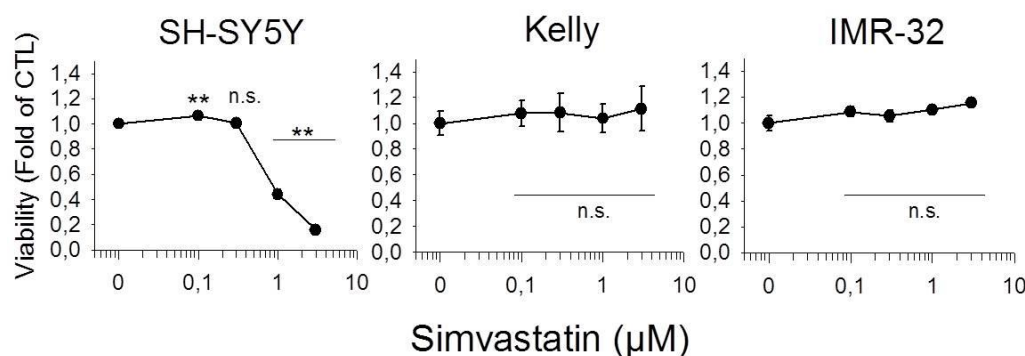
Figure 20: Viability of SH-SY5Y, Kelly and IMR-32 cells after 72 hours of simvastatin treatment.
Simvastatin was applied in concentrations from 0 to 3 µM. The results did show that simvastatin does not have a negative effect on the viability of Kelly and IMR-32 cell lines. But it brings down SH-SY5Y cell line. Results were analysed at 490 nm and at 655 nm served as reference measurement. Samples were all carried out as triplicates. The reference values were subtracted from the 490 nm values. Results represent the mean of fold of control values. Error bars denote SD; n.s. : not significant; n : 3

9.5.3 TAE684 is a promising new drug decreasing viability in SH-SY5Y, Kelly and IMR-32 cell lines

Three drugs, namely simvastatin, aurora kinase inhibitor VX680 and ALK inhibitor TAE684 were chosen to target viability of NB cells and drug combinations were compared with single compound efficacy. Simvastatin was applied in concentrations of 1µM in SH-SY5Y cells and 3 µM in Kelly and IMR-32 cells. For VX680 the concentration range from 0.1 nM to 30 nM was chosen according to previous experiments and for TAE684 the range from 0.1 nM to 1000 nM (Figure 21). All three cell lines were first cultured for 24 hours on 96 well plates before drug treatment and further incubation for 72 hours. All samples were applied as triplicates and the experiments were repeated at least twice. Results were evaluated as described in section 11.5 and data is expressed as fold of control.

In SH-SY5Y cells a simvastatin concentration of 1 µM was again proven to bring down about 60% of the cells. On the other hand VX680 applied in concentrations ranging from 0.1 nM to

30 nM did not show any effect in this cell line and viability did not change compared to the control samples. This leads to the result that neither additive no synergistic effects could be detected with the combination of VX680 0.1 nM to 30 nM with 1 µM simvastatin. The ALK inhibitor TAE684 showed similar impacts at a concentration of 100 nM as 1 µM simvastatin and about 50% of the cells could be killed with this drug. In combination with VX680 and simvastatin no synergy effects could be observed. When 0.1 nM to 1000 nM of TAE684 and 1 µM of simvastatin were combined however additive effects resulted and viability sunk to 10% to 20% in comparison to the untreated control. In Kelly cells again the VX680 aurora kinase inhibitor applied in concentrations from 0.1 nM to 3 nM did not affect cell viability.
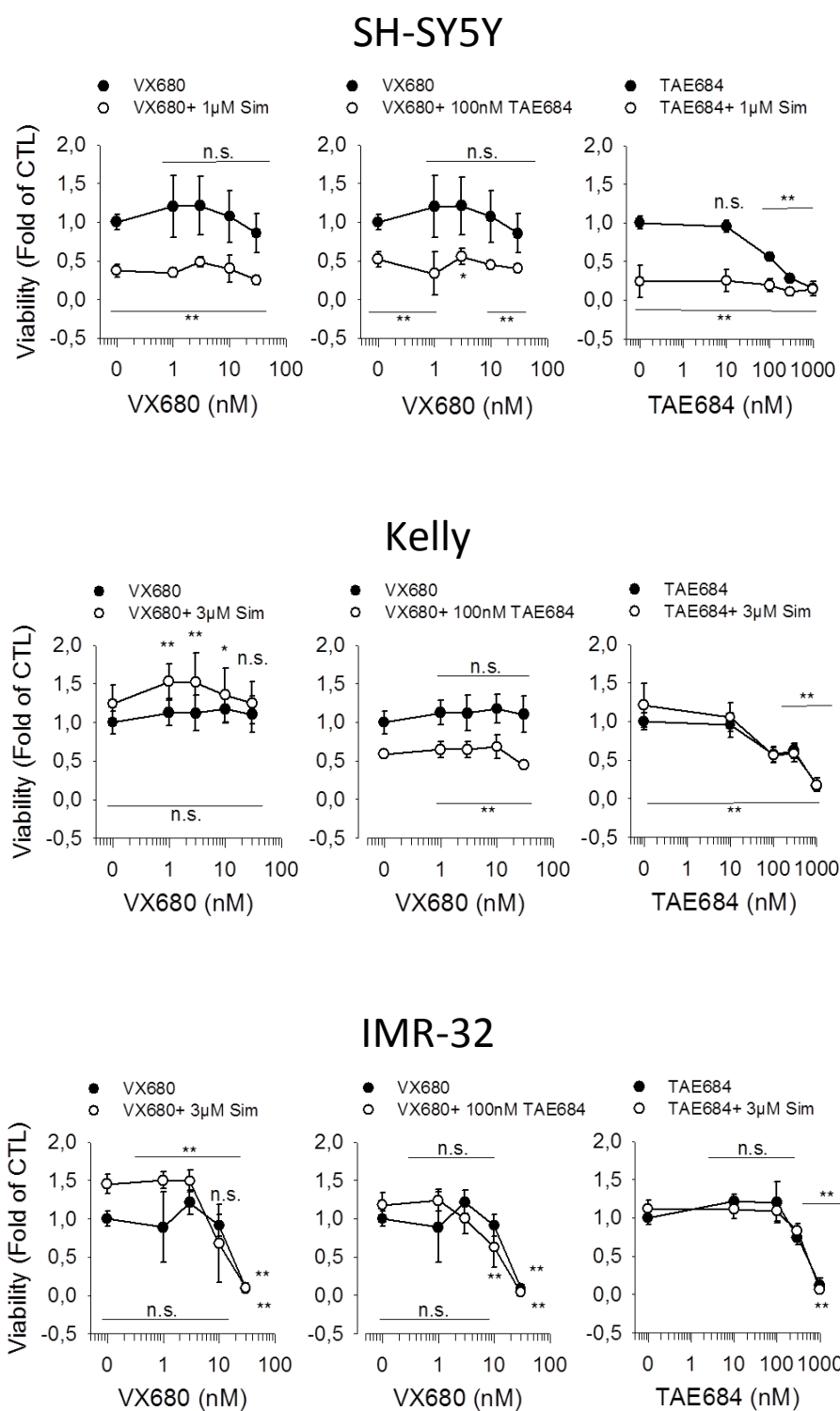
Figure 21: Viabilities of SH-SY5Y, Kelly and IMR-32 cell lines after treatments with VX680, TAE684, simvastatin and combinations.
SH-SY5Y, Kelly and IMR-32 cell lines were incubated with VX680, TAE684, simvastatin and the indicated combinations. The viability was monitored by MTT metabolization. Samples were all carried out as triplicates. Results represent the mean of fold of control values. Error bars denote SD; n.s. : not significant, * : $p<0.05$, ** : $p<0.05$; n = 6

Here simvastatin was applied in a higher concentration of 3 µM in comparison to the treatment of SH-SY5Y cells as Kelly and IMR-32 cells are known to be more resistant to this substance. But simvastatin at a concentration of 3 µM even caused an increase of viability of 20% to 50% in comparison to the control. The combination did not show an additional effect. 100 nM TAE684 could decrease the viability to 50% to 60% while again the combination of 100 nM and 0.1 nM to 30 nM VX680 did not lead to a change in viability compared to the control. The combination of TAE684 and 3µM simvastatin clearly shows that simvastatin could not further enhance cytotoxicity of TAE684.

Finally, in IMR-32 cells VX680 could negatively influence cell viability and could lead to only 10% of survival at the highest concentration of 30 nM. Simvastatin here again applied at a concentration of 3 µM did not affect cell viability and therefore it did not lead to neither additive nor synergy effects. And also TAE684 had the suspected impact on IMR-32 cells. Applied in concentrations from 0.1 nM to 1000 nM it was able to significantly reduce living cells to only 10% compared to the control.

To sum up, these viability assays revealed that VX680 could be effective against IMR-32 cells in concentrations higher than 3 nM. Nevertheless, it did not lead to convincing results in the other two cell lines. On the other hand, TAE684 was the outstanding substance of these experiments as it was able to induce cell death in all of the three cell lines. While in SH-SY5Y cells already 100 nM could decrease viability to about 50% in IMR-32 cells a higher concentration of about 500 nM is needed to lead to this result.

9.5.4 Results of viability assays accord with observations of cell morphology after drug treatment

The simvastatin effects examined by viability assays affirmed the morphological observations documented by microscopy (Figure 11 and Figure 20). Accordingly, morphology was also depicted for ALK and aurora kinase inhibition (Figure 22). For comparison again simvastatin led to a hardly noticeable change in morphology of Kelly and IMR-32 cells while the applied concentration of 3 µM did clearly affect morphology of SH-SY5Y cells.

VX680 at a concentration of 10 nM was only active in IMR-32 cells while SH-SY5Y and Kelly cells were not susceptible to reduced viability.

TAE684 was the only drug leading to cell death in all three cell lines which is documented also in the changes of the morphology. In Figure 22 cells treated with 200 nM and 2 µM of TAE684 are depicted. Images taken of cells that had been incubated with 200 nM of TAE684 might not show the effects as clearly as observed in viability assays. But the higher substance concentration of 2 µM reveals that it is very harmful for all three cell lines as nearly no cells survived this treatment. That is also why lower concentrations were chosen for further experiments to identify differences in dose-effect relation in the different cell types.
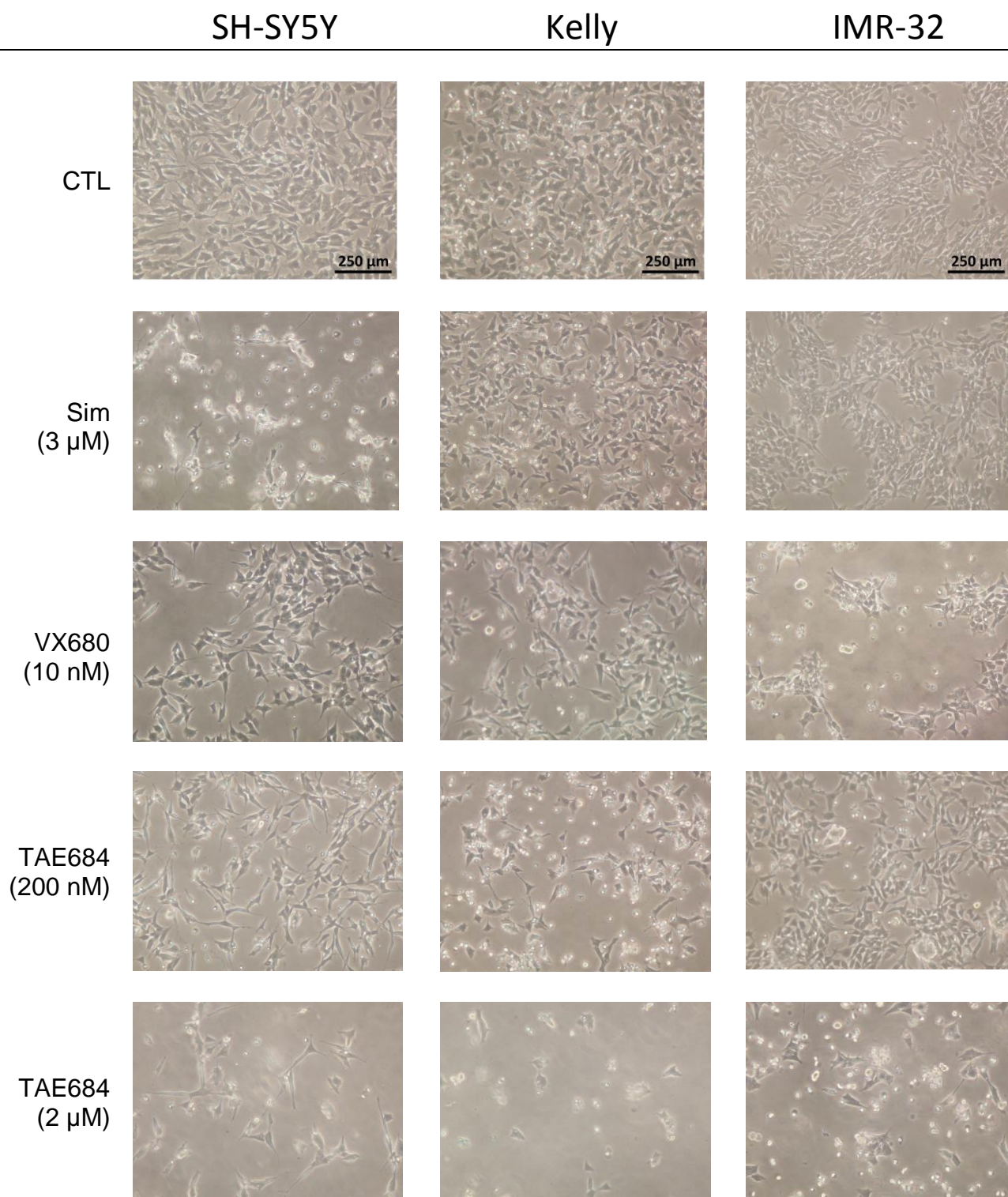
Figure 22: Morphologies of SH-SY5Y, Kelly and IMR-32 cell lines show heterogeneous changes after different drug treatments.
The three cell lines are shown when normally grown in cell culture (CTL) and after 48 hour treatments with 3 µM simvastatin (Sim), 10 nM VX680 aurora kinase inhibitor and 200 nM as well as 2 µM of ALK inhibitor TAE684. Scale bar = 250 µm

9.5.5 HDAC inhibitor trichostatin A did also decrease viability of SH-SY5Y, Kelly and IMR-32 cells

The HDAC inhibitor trichostatin A (TSA) was also tested for its effects on the three NB cell lines (Figure 23). After cells could grow for 24 hours on a 96 well plate TSA was applied in concentrations from 0.1 to 10 µM. The triplicate samples were then incubated for another 48 hours. Measurement was performed as described for all viability assays at the beginning of this chapter (section 11.5).

All three cell lines showed similar reactions to this substance. At the concentration of 0.1 µM already 30% of cells had died and with the highest concentration of 10 µM the survival decreased to only 10%. In Kelly cells 0.1 µM of TSA led to only 40% of survival and 10 µM nearly killed all cells as only 2% of cells could be detected. IMR-32 cells reacted more similarly to SH-SY5Y cells with 50% of survival after treatment with 0.1 µM and 10% survival after treatment with 10 µM of TSA.
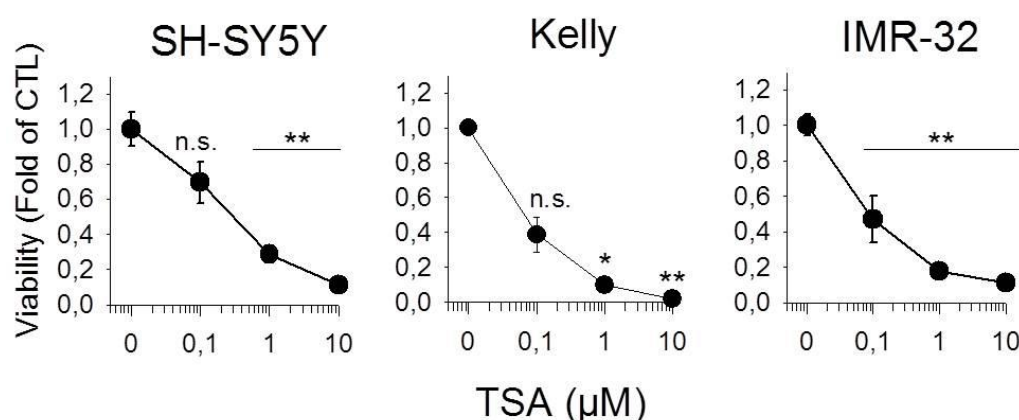
Figure 23: 10 µM HDAC inhibitor TSA decreased cell viability significantly in SH-SY5Y, Kelly and IMR-32 cells. Results were analysed at 490 nm and at 655 nm served as reference measurement. Samples were all carried out as triplicates. The reference values were subtracted from the 490 nm values. Results represent the mean of fold of control values. Error bars denote SD; n.s. : not significant, * : $p < 0.05$, ** : $p < 0.05$; n = 3

9.5.6 Tumour necrosis factor α did not cause cell death in SH-SY5Y´, Kelly and IMR-32 cells

Tumour necrosis factor α (TNFα) was applied as it is able to induce inflammatory events that can also induce cell death. Its effects on the three NB cell lines are shown in Figure 24. Cells were first allowed to grow for 24 hours on a 96 well plate before TNFα was applied in concentrations from 1 to 30 ng/ml. Samples were executed as triplicates and measurement was performed as described at the beginning of this chapter (section 11.5).

The treatment however did not lead to any significant change of viability compared to control samples in neither of the cell lines. NFκB is not activated by TNFα in Kelly and IMR-32 cells (see section 11.4 "NFκB luciferase reporter assay"). In SH-SY5Y cells a significant activation could be observed in luciferase reporter assay. However this effect is not related to TNFα induced changes in viability.
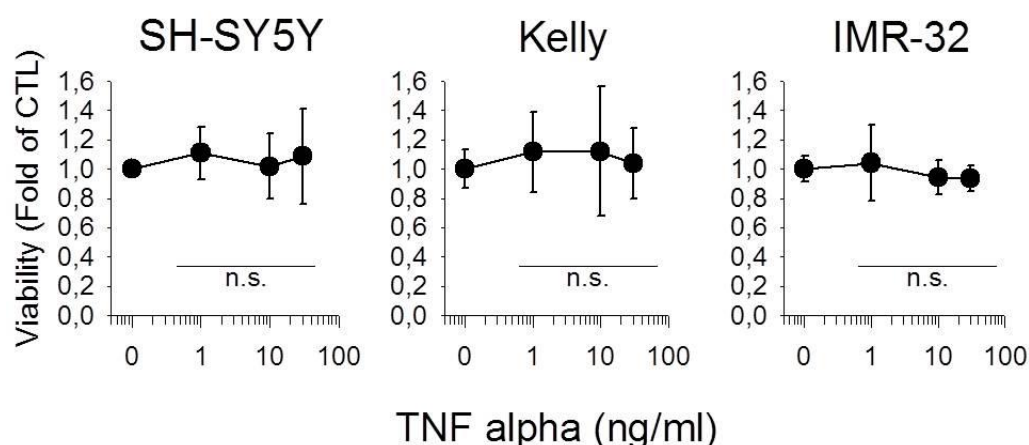
Figure 24: Treatment of SH-SY5Y, Kelly and IMR-32 cells with TNFα did not lead to a significant change of viability.
Results were analysed at 490 nm and at 655 nm served as reference measurement. Samples were all carried out as triplicates. The reference values were subtracted from the 490 nm values. Results represent the mean of fold of control values. Error bars denote SD; n.s. : not significant; n = 3

9.6 Western blot analysis for apoptotic markers after drug treatment

Viability assays already revealed different efficiencies for induction of cell death by various drugs. Another interest was to identify the way cell death was caused by the according drugs. This is the reason why Western blot analysis was applied to check for apoptotic pathway markers in treated SH-SY5Y, Kelly and IMR-32 cells.

Cells were cultured for 24 hours and then treated with the different substances. Control samples were not treated with any drug and were only supplied with the according growth medium.

9.6.1 Caspase 3 cleavage proves apoptotic events in SH-SY5Y cells treated with simvastatin

Caspases are enzymes with essential roles in apoptotic events described in further detail in the introduction (section 7.5). Caspase 3 is a key mediator of apoptosis and it is activated by cleavage by other caspases. This event introduces degradation of the cell. That is why Western blot analysis of total cell lysates was performed to screen for cleavaged pro-caspase 3.

Cells were treated for 48 hours with simvastatin alone at concentrations of 0.1, 0.3, 1 and 3 µM, with VX680 aurora kinase inhibitor at concentrations of 1 and 10 µM and TAE684 ALK inhibitor at concentrations of 20 and 200 nM (Figure 25). For detection caspase 3 rabbit polyclonal antibodies specific for the intact protein were employed. This antibody not only detects the intact protein at 35 kDa but also the cleavage fragments at 19 and 17 kDa. Simvastatin treatment showed caspase cleavage at 3 µM in SH-SY5Y cells why this concentration was chosen for combination treatments with VX680 and TAE684.
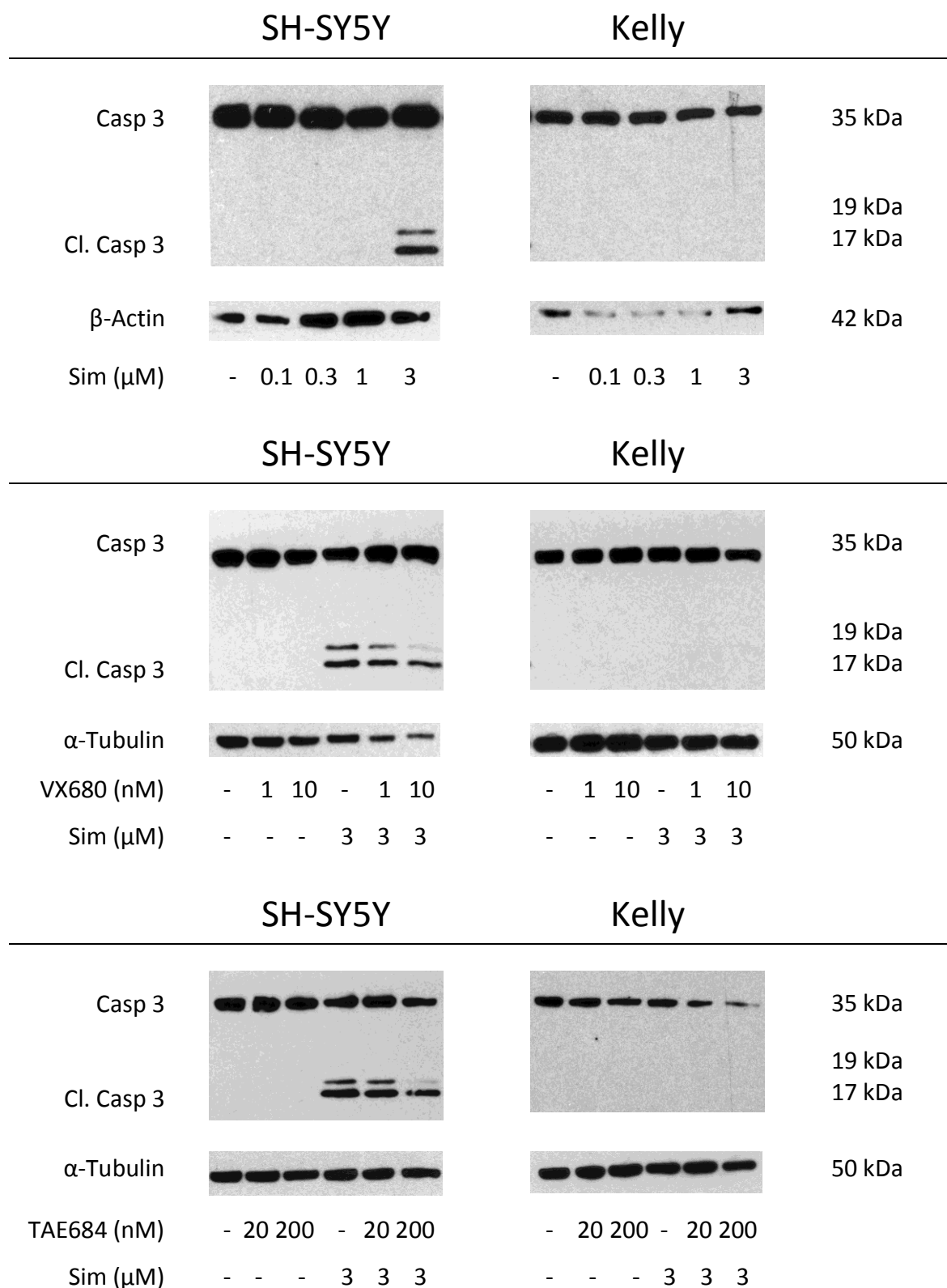
Figure 25: Caspase 3 cleavage in SH-SY5Y, Kelly and IMR-32 cells treated with 3 µM simvastatin.
Cells were incubated for 48 hours with simvastatin (Sim) 0.1 to 3 µM, 1 and 10 nM of VX680 and 20 and 200 nM of TAE684. Total cell lysates were employed for Western blots and detection was performed with caspase 3 intact protein (Casp 3, 35 kDa) that also allows detection of fragments (Cl. Casp 3, 19 and 17 kDa). Results are shown above with either β-Actin or α-Tubulin serving as loading controls.

All samples were at least tested twice. They are here depicted with either β-Actin or α-Tubulin as loading controls. In Figure 25 only Western blot results for SH-SY5Y and Kelly cells are shown. IMR-32 cells delivered the exact same results as Kelly cells, namely that no caspase 3 cleavage could be detected for none of the employed drugs and combinations with simvastatin. But a slight decrease of intensity regarding the intact protein at concentration of 200 nM of TAE684 is visible. Probably the cleaved fragment is too low of a concentration to be detectable. In SH-SY5Y cells simvastatin at the concentration of 3 μM was able to induce caspase 3 cleavage and the smaller fragments are clearly visible on the blots. But all the other substances did not cause caspase 3 cleavage in detectable concentrations.

9.6.2 PARP1 cleavage indicates apoptosis in SH-SY5Y cells incubated with simvastatin

Like described before and in more detail in section 7.5 "Apoptosis signalling pathways - targets for cancer therapy" caspase 3 is a key mediator of apoptosis. When activated it causes the degradation of cells by cleavage and inactivation of different other factors important for cell survival like for instance poly(ADP-ribose) polymerase1 (PARP1). This protein usually involved in DNA repair loses this capacity after being cleaved. PARP1 whole protein appears at 119 kDa and its cleaved fragment at 89 kDa and an additional small fragment at 24 kDa (not shown in the following figures).

Only SH-SY5Y cells were treated for 48 hours with simvastatin alone at concentrations of 0.1, 0.3, 1 and 3 μM (Figure 26) as the other cell lines were proven many times before to not be affected by this substance. Total protein lysates were employed for Western blot analysis. For detection PARP rabbit polyclonal antibodies specific for the intact protein were employed. Samples were at least analysed twice and they are here shown with β-Actin as loading controls.

When compared to the control a clear 89 kDa band is visible in the sample treated with 3 μM of simvastatin which confirms the results for caspase 3 cleavage shown above. Besides the 3 μM simvastatin sample also the lower concentration of 1 μM simvastatin seems to have induced apoptosis as a very light band appears at 89 kDa. All in all, simvastatin once again was proven to be an effective drug in SH-SY5Y cells causing apoptosis.

SH-SY5Y
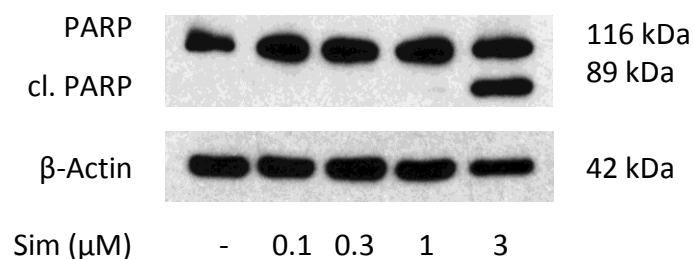
Figure 26: Simvastatin leads to PARP cleavage in SH-SY5Y cells.
Cells were treated with 0.1 to 3 µM simvastatin (Sim) for 48 hours. Total cell lysates were analysed. PARP total protein appears at 116 kDa (PARP) and fragments of 89 kDa indicate apoptosis (cl. PARP). Both were detected with PARP intact specific antibodies. β-Actin served as loading control.

9.6.3   Apoptosis by PARP1 cleavage in IMR-32 cells after treatment with VX680

PARP cleavage was also examined for the other substances and combinations with simvastatin. Cells were treated for 48 hours with 1 and 10 nM of VX680 before total cell lysis. Also combinations of the aurora kinase inhibitor with 3 µM simvastatin were applied. Samples were analysed at least twice and results are shown below in Figure 27. Detection was performed as described in section 11.6.2.
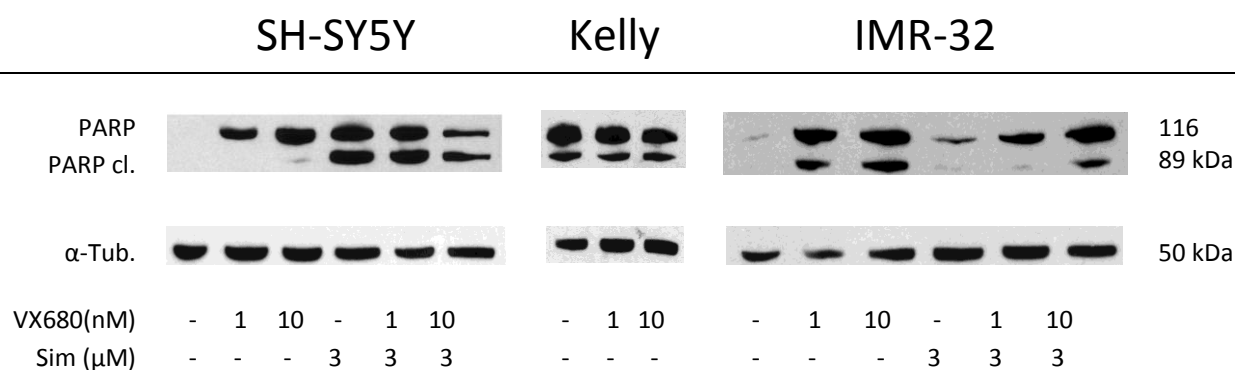
Figure 27: PARP cleavage in SH-SY5Y, Kelly and IMR-32 cells treated with VX680 and simvastatin.
VX680 was applied in concentrations of 1 and 10 nM and simvastatin (Sim) with a concentration of 3 µM. Cells were incubated for 48 hours. Total cell lysates were employed for analysis. α-Tubulin (α-Tub.) is depicted as loading control. PARP intact Protein appears at 116 kDa (PARP) and the cleaved fragment at 89 kDa (cl. PARP).

In SH-SY5Y cell line 3 µM of simvastatin is proven another time to induce apoptosis. Interestingly, 10 nM of VX680 led to a slight cleavage of PARP indicated by a very thin protein band at 89 kDa.

Kelly cell line was only treated with VX680 and not with additional simvastatin as it was proven to not affect this cell line in viability assays. And it is clearly recognizable that this drug does not lead to additional PARP cleavage compared to the control as already in the control sample there is a distinct amount of cleaved 89 kDa fragment detectable.

In IMR-32 cell line VX680 increases the cleavage of PARP protein more clearly visible in the combination samples with simvastatin.

9.6.4 TAE684 induces apoptosis in SH-SY5Y, Kelly and IMR-32 cells

Proteins of the three NB cell lines were also treated for 48 hours with 20 and 200 nM of TAE684 and checked for PARP cleavage. Combinations of the ALK inhibitor with 3 µM simvastatin were applied, too. All samples were examined at least twice and results are depicted in Figure 28. Detection was performed as described in section 11.6.2.
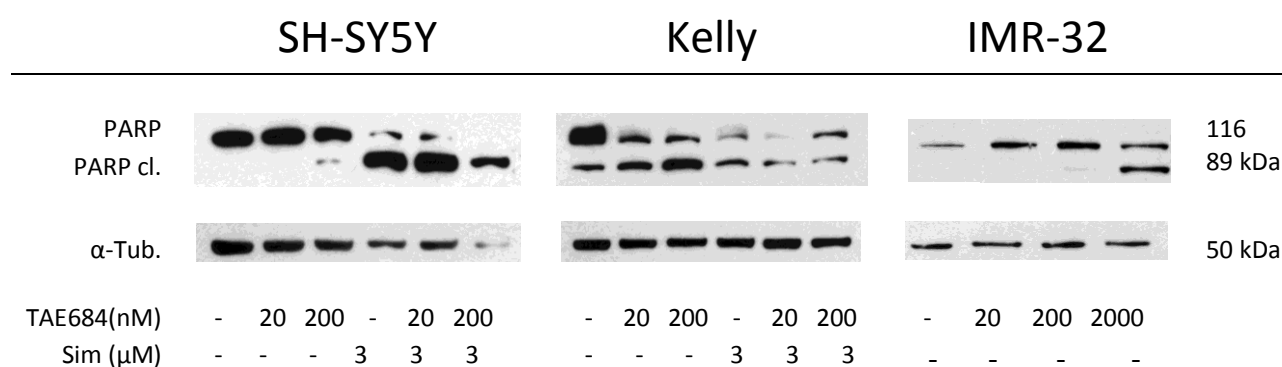
Figure 28: PARP cleavage after TAE684 treatment in SH-SY5Y, Kelly and IMR-32 cell lines.
TAE684 was applied in concentrations of 20 and 200 nM and simvastatin (Sim) with a concentration of 3 µM. Cells were incubated for 48 hours. Total cell lysates were employed for analysis. α-Tubulin (α-Tub.) is depicted as loading control. PARP intact Protein appears at 116 kDa (PARP) and the cleaved fragment at 89 kDa (cl. PARP).

SH-SY5Y cells clearly show an intact PARP protein at 116 kDa after treatment with 200 nM TAE684. This is also consistent with results from viability assays. Of course an additional simvastatin concentration of 3 µM induces PARP cleavage at a large quantity. In the highest concentration of TAE684 and simvastatin there is no more intact PARP protein detectable.

In Kelly cells PARP cleavage is already present in the control sample as observed before but one can clearly recognize the increase of the cleaved PARP fragment of 89 kDa with higher TAE684 concentrations. This again is proof for the effectiveness of TAE684 in this cell line.

Proteins of IMR-32 cells only depicted after TAE684 treatment alone do very nicely illustrate how intact PARP protein concentration lowers while the band indicating the smaller PARP fragment becomes more clearly visible. As also in IMR-32 cells cell death by apoptosis is induced by TAE684 all three cell lines are again proven to be affected by this substance.

10 Discussion

MYCN amplification has been described as one of the rare consistent genetic markers in NB that is correlated with poor prognosis for the patient.[9,10] High N-Myc levels contribute to mis-regulation of the cell cycle of neuroblasts.[27] The pathway proposed by Otto *et al.* is depicted in an adapted manner in Figure 29 (see also section 6.2.3 "N-Myc in NB and therapeutic opportunities" for more details). While in un-transformed neuroblast development N-Myc degradation allows neuroblasts to exit cell cycle, in malignant development however N-Myc concentrations are kept high. Various compounds are believed to participate in the process of N-Myc protein stabilization and they are considered promising targets for pharmacological intervention against this malignant disease.

The main goal of this study was to investigate the pharmacological potential of various selected drugs that partly have already been introduced into clinical trials. The conducted experiments aimed to test the effects of the substances alone on viability and apoptotic events in three NB cell lines. Furthermore drugs were applied in double combinations for identification of additional effects and possible synergy effects.
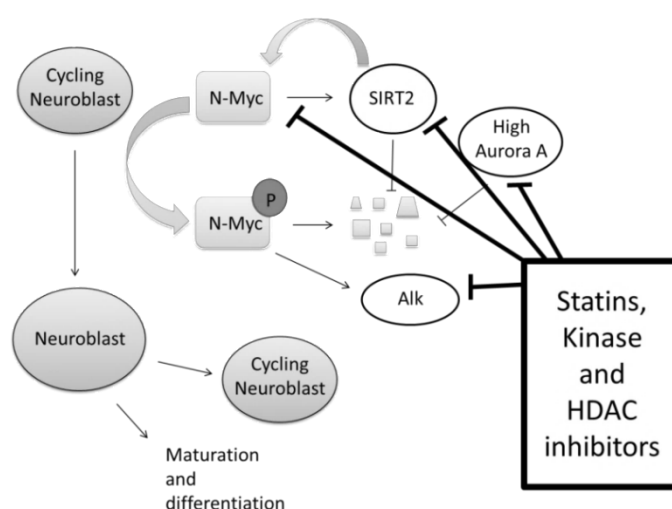
Figure 29: High levels of N-Myc protein keep neuroblasts in proliferative state.
Statins, aurora kinase A and ALK inhibitors as well as HDAC inhibitors were employed to investigate the effects on viability and apoptosis of three neuroblastoma cell lines.

10.1 Simvastatin alone inhibits viability of SH-SY5Y but does not affect Kelly and IMR-32 cells

SH-SY5Y cells reveal their susceptibility to simvastatin already in cell culture and with low concentrations between 1 and 3 µM. Kelly and IMR-32 cells on the other hand do not change in morphology after treatment (Figure 11 and Figure 22). This observation is confirmed with viability assay results (Figure 20 and Figure 21). Simvastatin in concentrations from 0.1 to 3 µM does not change viability in Kelly and IMR-32 cells at all while viability in SH-SY5Y cells is significantly decreased with an IC_{50} of 0,64 µM ± 0,25 µM. Furthermore, similar effects are shown in Western blot analysis with antibodies specific for caspase 3 and PARP cleavage revealing apoptotic events. In simvastatin treated Kelly and IMR-32 cells cleavage of the two apoptotic markers is not detectable. But SH-SY5Y cells already show caspase 3 cleavage after treatment with 3 µM of the substance and PARP cleavage already starting to appear at concentrations of 1 µM simvastatin (Figure 25, Figure 26, Figure 27 and Figure 28).

10.2 VX680 brings down IMR-32 cells

Aurora kinase A inhibitor VX680 was one of the chosen substances to test in combination experiments with simvastatin (Figure 21). Interestingly viability in SH-SY5Y and Kelly cells is not affected with this substance at concentrations of 1 to 30 nM. IMR-32 cell line however is on the other hand susceptible to VX680 with an IC_{50} of 10,83 nM ± 0,77 nM. In combination experiments no additional or synergy effects could be revealed. Western blot analysis for apoptosis marker caspase 3 and PARP verified these findings (Figure 25 and Figure 27). While caspase cleavage is not shown for IMR-32 cells in Kelly and SH-SY5Y cells caspase is not cleaved indicating no apoptosis. PARP cleavage however is detectable in IMR-32 cells treated with VX680.

10.3 TAE684: potential new substance against neuroblastoma cells

The second substance chosen for combination treatment with simvastatin was ALK inhibitor TAE684. It is able to lower viability in all three cell lines with an IC_{50} of 99,92 nM ± 0,18 nM in SH-SY5Y, 58,74 nM ± 0,1 nM in Kelly cells and 388 nM ± 0,1 nM in IMR-32 cells (Figure 21). Although no additional or synergy effects in combination with simvastatin are revealed still this is a convincing finding. In Western blot analysis however caspase 3 cleavage is not detected for any of the cell lines but PARP cleavage clearly increases with TAE684 treatment (Figure 25 and Figure 28).

10.4 VX680 combined with TAE684

The combination of the two kinase inhibitors VX680 and TAE684 did not show additional or synergy effects. Nevertheless, the results described above could be confirmed with these experiments (Figure 21).

10.5 General discussion

HMG-CoA reductase inhibitor simvastatin, aurora kinase A inhibitor VX680, anaplastic lymphoma kinase (ALK) inhibitor TAE684 and histone deacetylase (HDAC) inhibitor trichostatin A (TSA) were chosen as compounds tested in the experiments due to different data and findings from previous studies and publications.

Statins are commonly prescribed against cardiovascular diseases but they are also known for their pleiotropic effects (see section 6.3 "Statins and their pleiotropic effects"). Among others they were proven to be effective against different cancer types like human melanoma, rhabdomyosarcoma and neuroblastoma SH-SY5Y cells.[69-72] In this study simvastatin could be confirmed again as a striking agent decreasing the viability of SH-SY5Y cells tremendously but barely having an effect on the MYCN amplified cell lines. MYCN gene amplification and high N-Myc protein levels have been established as markers for more advanced NB stages

and patients with poor future outcome.[9,10] In this study MYCN amplification in Kelly and IMR-32 cell lines compared to the control cell line SH-SY5Y without amplification is confirmed on genetic levels by PCR analysis of total cell RNA isolates with MYCN specific primers and employment of the same cDNA concentrations for all three cell lines. Results are shown in Figure 12 revealing lower concentrations of MYCN RNA present in SH-SY5Y cells than Kelly cells which are followed by IMR-32 cells. Moreover amplification is verified by Western blot analysis of total cell lysates with N-Myc specific antibodies (Figure 13). While N-Myc protein is hardly detectable under the same conditions Kelly and IMR-32 cells show clear dark bands for the protein. Although these results affirm the higher presence of MYCN RNA and N-Myc proteins in Kelly and IMR-32 cells this does not clarify the mechanisms and regulations by which N-Myc concentrations are kept high. Further investigations for components by which protein degradation is impaired or for screening of proteins that influence N-Myc stability could provide more information. In addition the mechanisms how MYCN amplified cells become unsusceptible or less susceptible to simvastatin remain elusive and would have to be further investigated. Obstruction of these defensive pathways would allow treatment of these cells with statins and would make new applications possible.

Another promising new targeted strategy for cancer treatment is aurora kinase A inhibition. Aurora kinase A is a crucial factor in the process of mitosis and de-regulations have been identified in different cancer types such as colorectal, gastric, prostate and breast cancer.[74,75] Aurora kinase A inhibitor VX680 was chosen as drug for the experiments as aurora kinase A inhibitors have been reported to regulate N-Myc metabolism.[27] Besides, aurora kinase A amplifications and mutations are considered other negative prognostic features in NB.[22,27] In this study however viability could only be decreased in one cell line, IMR-32. Aurora kinase A inhibitor needs the proapoptotic pathways to be activated and the mitosis process to be enduring for making an impact.[75] An explanation could be that IMR-32 cells were observed to be much slower in cell division and proliferation compared to the other two cell lines during all the experiments therefore they may be more susceptible to this substance. Furthermore the employment of aurora kinase inhibitors in combination with mitosis prolonging factors could also allow the treatment of the other cell lines.

In addition, this study provides evidence that TAE684 ALK inhibitor is an effective drug against not only SH-SY5Y but also against the MYCN amplified Kelly and IMR-32 cell lines.

Anaplastic lymphoma kinase gene encodes a receptor tyrosine kinase and when present in high concentrations it was stated to be associated with poor prognosis for NB patients even without ALK mutations present.[76] ALK mutation and amplification however are correlated with MYCN amplification and define a high risk patient.[77] In *in vitro* trials different NB cell lines were found to have various susceptibilities to the ALK inhibitor TAE684.[76,78] They revealed that cells in possession of ALK mutations, mostly gain of function mutations, were more sensitive to the substance. As SH-SY5Y and Kelly cells are both indeed in the possession of the F1174L mutations the successful inhibition of growth by TAE684 is not surprising and was already tested in previous studies.[78] In contrast IMR-32 is in the possession of the wild-type receptor and therefore much less sensitive to the substance.[79]

Another approach for cancer therapy is to target not the tumour cells themselves but the tumour microenvironment. It has been known for a long time that chronic inflammation can be involved in cancer formation. Inflammatory cells are present in proximity to solid tumours (see also section 6.4 "NFκB- A link between inflammation and cancer") responding to cell damages.[80] That is why experiments regarding activation of NFκB activity were performed by employing a luciferase gene reporter assay. For the conduction of the gene reporter assay one needs an effective transfection method. As especially MYCN amplified human NB cell lines are well known to be challengeable to transfect first a broad spectrum of tools were tested and methods compared (Figure 15 and Figure 16). The K2® reagent by Biontex is able to achieve comparable transfection efficiencies for all three cell lines and is therefore the ideal compound for following experiments. After the discovery that all three tested cell lines are not divergent in their basal NFκB activity (data not shown) they were treated with TNFα, simvastatin and TSA (Figure 17). TNFα could only show significant stimulation of NFκB in SH-SY5Y cells in which cell line on the other hand simvastatin was able to block NFκB transcription activity. While in IMR-32 cells none of the results were significant in Kelly cells TSA led to significant increase of NFκB activity. This data however could not deliver an explanation for the strong inhibition of viability by TSA (Figure 23).

Targeting epigenetic alterations would be a further possibility of treatment in cancer and NB in particular. Histone deacetylase SIRT2 has been shown to promote stability of N-Myc protein.[81] This is the reason for the employment of HDAC inhibitor TSA.

11 Conclusion

This study proves again the high susceptibility of SH-SY5Y cells to simvastatin and its ability of inducing apoptosis in this cell line. MYCN amplified cell lines however are not negatively affected by this drug according to my results. Nevertheless, the aurora kinase A inhibitor VX680 is shown to reduce viability in IMR-32 cells and the ALK inhibitor TAE684 is effective in all the three cell lines. In order to identify in particular the resistance mechanism toward simvastatin in IMR-32 and Kelly cells will open a new window to approach therapeutic targeting of these highly malignant cell types. Further studies will reveal more insights about pathways and functions in these cells allowing more accurately and therefore more successful treatments also in patients.

12 List of Figures

13 List of Tables

14 References

1.   Bell, E., *et al.* MYCN oncoprotein targets and their therapeutic potential. *Cancer letters* **293**, 144-157 (2010).

2.   Weinstein, J.L., Katzenstein, H.M. & Cohn, S.L. Advances in the diagnosis and treatment of neuroblastoma. *The oncologist* **8**, 278-292 (2003).

3.   Bordbar, M., Tasbihi, M., Kamfiroozi, R. & Haghpanah, S. Epidemiological and clinical characteristics of neuroblastoma in southern iran. *Iranian journal of pediatric hematology and oncology* **4**, 89-96 (2014).

4.   Schwab, M., Westermann, F., Hero, B. & Berthold, F. Neuroblastoma: biology and molecular and chromosomal pathology. *The Lancet. Oncology* **4**, 472-480 (2003).

5.   Owens, C. & Irwin, M. Neuroblastoma: the impact of biology and cooperation leading to personalized treatments. *Critical reviews in clinical laboratory sciences* **49**, 85-115 (2012).

6.   Maris, J.M. Recent advances in neuroblastoma. *N Engl J Med* **362**, 2202-2211 (2010).

7.   Brodeur, G.M., *et al.* Revisions of the international criteria for neuroblastoma diagnosis, staging, and response to treatment. *Journal of clinical oncology : official journal of the American Society of Clinical Oncology* **11**, 1466-1477 (1993).

8.   Monclair, T., *et al.* The International Neuroblastoma Risk Group (INRG) staging system: an INRG Task Force report. *Journal of clinical oncology : official journal of the American Society of Clinical Oncology* **27**, 298-303 (2009).

9.   Brodeur, G.M. & Bagatell, R. Mechanisms of neuroblastoma regression. *Nature reviews. Clinical oncology* **11**, 704-713 (2014).

10.   Brodeur, G.M. Neuroblastoma: biological insights into a clinical enigma. *Nature reviews. Cancer* **3**, 203-216 (2003).

11.   Nakagawara, A., *et al.* Association between high levels of expression of the TRK gene and favorable outcome in human neuroblastoma. *N Engl J Med* **328**, 847-854 (1993).

12.   Cohn, S.L. & Tweddle, D.A. MYCN amplification remains prognostically strong 20 years after its "clinical debut". *Eur J Cancer* **40**, 2639-2642 (2004).

13.   Perez, C.A.*, et al.* Biologic variables in the outcome of stages I and II neuroblastoma treated with surgery as primary therapy: a children's cancer group study. *Journal of clinical oncology : official journal of the American Society of Clinical Oncology* **18**, 18-26 (2000).

14.   Bowman, L.C.*, et al.* Genetic staging of unresectable or metastatic neuroblastoma in infants: a Pediatric Oncology Group study. *J Natl Cancer Inst* **89**, 373-380 (1997).

15.   Matthay, K.K.*, et al.* Patterns of relapse after autologous purged bone marrow transplantation for neuroblastoma: a Childrens Cancer Group pilot study. *Journal of clinical oncology : official journal of the American Society of Clinical Oncology* **11**, 2226-2233 (1993).

16.   Matthay, K.K.*, et al.* Treatment of high-risk neuroblastoma with intensive chemotherapy, radiotherapy, autologous bone marrow transplantation, and 13-cis-retinoic acid. Children's Cancer Group. *N Engl J Med* **341**, 1165-1173 (1999).

17.   Sidell, N., Altman, A., Haussler, M.R. & Seeger, R.C. Effects of retinoic acid (RA) on the growth and phenotypic expression of several human neuroblastoma cell lines. *Experimental cell research* **148**, 21-30 (1983).

18.   Lautz, T.B., Naiditch, J.A., Clark, S., Chu, F. & Madonna, M.B. Efficacy of class I and II vs class III histone deacetylase inhibitors in neuroblastoma. *Journal of pediatric surgery* **47**, 1267-1271 (2012).

19.   Evans, A.E.*, et al.* Antitumor activity of CEP-751 (KT-6587) on human neuroblastoma and medulloblastoma xenografts. *Clinical cancer research : an official journal of the American Association for Cancer Research* **5**, 3594-3602 (1999).

20.   Hoefnagel, C.A., De Kraker, J., Valdes Olmos, R.A. & Voute, P.A. [131I]MIBG as a first line treatment in advanced neuroblastoma. *Q J Nucl Med* **39**, 61-64 (1995).

21.   Mackall, C.L., Merchant, M.S. & Fry, T.J. Immune-based therapies for childhood cancer. *Nature reviews. Clinical oncology* **11**, 693-703 (2014).

22.   Hasan, M.K.*, et al.* ALK is a MYCN target gene and regulates cell migration and invasion in neuroblastoma. *Scientific reports* **3**, 3450 (2013).

23.   Galkin, A.V.*, et al.* Identification of NVP-TAE684, a potent, selective, and efficacious inhibitor of NPM-ALK. *Proceedings of the National Academy of Sciences of the United States of America* **104**, 270-275 (2007).

24.   Schulte, J.H.*, et al.* Targeted Therapy for Neuroblastoma: ALK Inhibitors. *Klinische Padiatrie* **225**, 303-308 (2013).

25.   Michaelis, M.*, et al.* Aurora kinases as targets in drug-resistant neuroblastoma cells. *PloS one* **9**, e108758 (2014).

26.   Shang, X.*, et al.* Aurora A is a negative prognostic factor and a new therapeutic target in human neuroblastoma. *Molecular cancer therapeutics* **8**, 2461-2469 (2009).

27.   Otto, T.*, et al.* Stabilization of N-Myc is a critical function of Aurora A in human neuroblastoma. *Cancer cell* **15**, 67-78 (2009).

28.   Roussel, M.*, et al.* Three new types of viral oncogene of cellular origin specific for haematopoietic cell transformation. *Nature* **281**, 452-455 (1979).

29.   Collins, S. & Groudine, M. Amplification of endogenous myc-related DNA sequences in a human myeloid leukaemia cell line. *Nature* **298**, 679-681 (1982).

30.   Alitalo, K., Schwab, M., Lin, C.C., Varmus, H.E. & Bishop, J.M. Homogeneously staining chromosomal regions contain amplified copies of an abundantly expressed cellular oncogene (c-myc) in malignant neuroendocrine cells from a human colon carcinoma. *Proceedings of the National Academy of Sciences of the United States of America* **80**, 1707-1711 (1983).

31.   Schwab, M.*, et al.* Amplified DNA with limited homology to myc cellular oncogene is shared by human neuroblastoma cell lines and a neuroblastoma tumour. *Nature* **305**, 245-248 (1983).

32.   Nau, M.M.*, et al.* L-myc, a new myc-related gene amplified and expressed in human small cell lung cancer. *Nature* **318**, 69-73 (1985).

33.   Conacci-Sorrell, M., McFerrin, L. & Eisenman, R.N. An overview of MYC and its interactome. *Cold Spring Harbor perspectives in medicine* **4**, a014357 (2014).

34.   Cascon, A. & Robledo, M. MAX and MYC: a heritable breakup. *Cancer research* **72**, 3119-3124 (2012).

35.   Hopewell, R. & Ziff, E.B. The nerve growth factor-responsive PC12 cell line does not express the Myc dimerization partner Max. *Molecular and cellular biology* **15**, 3470-3478 (1995).

36.   Roussel, M.F. & Robinson, G.W. Role of MYC in Medulloblastoma. *Cold Spring Harbor perspectives in medicine* **3**(2013).

37. Gregory, M.A. & Hann, S.R. c-Myc proteolysis by the ubiquitin-proteasome pathway: stabilization of c-Myc in Burkitt's lymphoma cells. *Molecular and cellular biology* **20**, 2423-2435 (2000).

38. Dang, C.V. MYC on the path to cancer. *Cell* **149**, 22-35 (2012).

39. Dominguez-Sola, D.*, et al.* Non-transcriptional control of DNA replication by c-Myc. *Nature* **448**, 445-451 (2007).

40. Conacci-Sorrell, M., Ngouenet, C. & Eisenman, R.N. Myc-nick: a cytoplasmic cleavage product of Myc that promotes alpha-tubulin acetylation and cell differentiation. *Cell* **142**, 480-493 (2010).

41. Dang, C.V.*, et al.* The c-Myc target gene network. *Seminars in cancer biology* **16**, 253-264 (2006).

42. Zeller, K.I.*, et al.* Global mapping of c-Myc binding sites and target gene networks in human B cells. *Proceedings of the National Academy of Sciences of the United States of America* **103**, 17834-17839 (2006).

43. Brockmann, M.*, et al.* Small molecule inhibitors of Aurora-a induce proteasomal degradation of N-myc in childhood neuroblastoma. *Cancer cell* **24**, 75-89 (2013).

44. Sjostrom, S.K., Finn, G., Hahn, W.C., Rowitch, D.H. & Kenney, A.M. The Cdk1 complex plays a prime role in regulating N-myc phosphorylation and turnover in neural precursors. *Developmental cell* **9**, 327-338 (2005).

45. Goldstein, J.L. & Brown, M.S. Regulation of the mevalonate pathway. *Nature* **343**, 425-430 (1990).

46. Weitz-Schmidt, G. Statins as anti-inflammatory agents. *Trends in pharmacological sciences* **23**, 482-486 (2002).

47. Garcia-Roman, N., Alvarez, A.M., Toro, M.J., Montes, A. & Lorenzo, M.J. Lovastatin induces apoptosis of spontaneously immortalized rat brain neuroblasts: involvement of nonsterol isoprenoid biosynthesis inhibition. *Molecular and cellular neurosciences* **17**, 329-341 (2001).

48. Gazzerro, P.*, et al.* Pharmacological actions of statins: a critical appraisal in the management of cancer. *Pharmacological reviews* **64**, 102-146 (2012).

49. Kaneta, S., Satoh, K., Kano, S., Kanda, M. & Ichihara, K. All hydrophobic HMG-CoA reductase inhibitors induce apoptotic death in rat pulmonary vein endothelial cells. *Atherosclerosis* **170**, 237-243 (2003).

50.	Kwak, B., Mulhaupt, F., Myit, S. & Mach, F. Statins as a newly recognized type of immunomodulator. *Nature medicine* **6**, 1399-1402 (2000).

51.	Girardi, G. Can statins prevent pregnancy complications? *Journal of reproductive immunology* **101-102**, 161-167 (2014).

52.	Li, T.*, et al.* Effects of atorvastatin on the inflammation regulation and elimination of subdural hematoma in rats. *Journal of the neurological sciences* **341**, 88-96 (2014).

53.	Bonovas, S. Statins: do they have a potential role in cancer prevention and modifying cancer-related outcomes? *Drugs* **74**, 1841-1848 (2014).

54.	Sehdev, A.*, et al.* The role of statins for primary prevention in non-elderly colorectal cancer patients. *Anticancer research* **34**, 5043-5050 (2014).

55.	Thurnher, M., Nussbaumer, O. & Gruenbacher, G. Novel aspects of mevalonate pathway inhibitors as antitumor agents. *Clinical cancer research : an official journal of the American Association for Cancer Research* **18**, 3524-3531 (2012).

56.	Hoesel, B. & Schmid, J.A. The complexity of NF-kappaB signaling in inflammation and cancer. *Molecular cancer* **12**, 86 (2013).

57.	Hoffmann, A. & Baltimore, D. Circuitry of nuclear factor kappaB signaling. *Immunological reviews* **210**, 171-186 (2006).

58.	Fan, Y., Mao, R. & Yang, J. NF-kappaB and STAT3 signaling pathways collaboratively link inflammation to cancer. *Protein & cell* **4**, 176-185 (2013).

59.	Razani, B., Reichardt, A.D. & Cheng, G. Non-canonical NF-kappaB signaling activation and regulation: principles and perspectives. *Immunological reviews* **244**, 44-54 (2011).

60.	Wertz, I.E. & Dixit, V.M. Signaling to NF-kappaB: regulation by ubiquitination. *Cold Spring Harbor perspectives in biology* **2**, a003350 (2010).

61.	Colotta, F., Allavena, P., Sica, A., Garlanda, C. & Mantovani, A. Cancer-related inflammation, the seventh hallmark of cancer: links to genetic instability. *Carcinogenesis* **30**, 1073-1081 (2009).

62.	DiDonato, J.A., Mercurio, F. & Karin, M. NF-kappaB and the link between inflammation and cancer. *Immunological reviews* **246**, 379-400 (2012).

63.   Krammer, P.H., Kaminski, M., Kiessling, M. & Gulow, K. No life without death. *Advances in cancer research* **97**, 111-138 (2007).

64.   Wen, X., Lin, Z.Q., Liu, B. & Wei, Y.Q. Caspase-mediated programmed cell death pathways as potential therapeutic targets in cancer. *Cell proliferation* **45**, 217-224 (2012).

65.   Sayers, T.J. Targeting the extrinsic apoptosis signaling pathway for cancer therapy. *Cancer immunology, immunotherapy : CII* **60**, 1173-1180 (2011).

66.   Friedlander, R.M. Apoptosis and caspases in neurodegenerative diseases. *N Engl J Med* **348**, 1365-1375 (2003).

67.   Hengartner, M.O. The biochemistry of apoptosis. *Nature* **407**, 770-776 (2000).

68.   Demierre, M.F., Higgins, P.D., Gruber, S.B., Hawk, E. & Lippman, S.M. Statins and cancer prevention. *Nature reviews. Cancer* **5**, 930-942 (2005).

69.   Werner, M., Atil, B., Sieczkowski, E., Chiba, P. & Hohenegger, M. simvastatin-induced compartmentalisation of doxorubicin sharpens up nuclear topoisomerase II inhibition in human rhabdomyosarcoma cells. *Naunyn-Schmiedeberg's archives of pharmacology* **386**, 605-617 (2013).

70.   Werner, M., Sacher, J. & Hohenegger, M. Mutual amplification of apoptosis by statin-induced mitochondrial stress and doxorubicin toxicity in human rhabdomyosarcoma cells. *British journal of pharmacology* **143**, 715-724 (2004).

71.   Wasinger, C.*, et al.* Autocrine secretion of 15d-PGJ2 mediates simvastatin-induced apoptotic burst in human metastatic melanoma cells. *British journal of pharmacology* **171**, 5708-5727 (2014).

72.   Marcuzzi, A.*, et al.* Lovastatin-induced apoptosis is modulated by geranylgeraniol in a neuroblastoma cell line. *International journal of developmental neuroscience : the official journal of the International Society for Developmental Neuroscience* **30**, 451-456 (2012).

73.   Makela, T.P., Saksela, K. & Alitalo, K. Two N-myc polypeptides with distinct amino termini encoded by the second and third exons of the gene. *Molecular and cellular biology* **9**, 1545-1552 (1989).

74.   Hara, J. Development of treatment strategies for advanced neuroblastoma. *International journal of clinical oncology* **17**, 196-203 (2012).

75. Hilton, J.F. & Shapiro, G.I. Aurora kinase inhibition as an anticancer strategy. *Journal of clinical oncology : official journal of the American Society of Clinical Oncology* **32**, 57-59 (2014).

76. Duijkers, F.A.*, et al.* Anaplastic lymphoma kinase (ALK) inhibitor response in neuroblastoma is highly correlated with ALK mutation status, ALK mRNA and protein levels. *Cell Oncol (Dordr)* **34**, 409-417 (2011).

77. Grande, E., Bolos, M.V. & Arriola, E. Targeting oncogenic ALK: a promising strategy for cancer treatment. *Molecular cancer therapeutics* **10**, 569-579 (2011).

78. George, R.E.*, et al.* Activating mutations in ALK provide a therapeutic target in neuroblastoma. *Nature* **455**, 975-978 (2008).

79. Mazot, P.*, et al.* Internalization and down-regulation of the ALK receptor in neuroblastoma cell lines upon monoclonal antibodies treatment. *PloS one* **7**, e33581 (2012).

80. Landskron, G., De la Fuente, M., Thuwajit, P., Thuwajit, C. & Hermoso, M.A. Chronic inflammation and cytokines in the tumor microenvironment. *Journal of immunology research* **2014**, 149185 (2014).

81. Liu, P.Y.*, et al.* The histone deacetylase SIRT2 stabilizes Myc oncoproteins. *Cell death and differentiation* **20**, 503-514 (2013).